© 2023. Published by The Company of Biologists Ltd | Development (2023) 150, dev201391. doi:10.1242/dev.201391

STEM CELLS AND REGENERATION

RESEARCH ARTICLE

Hox genes are crucial regulators of periosteal stem cell identity

Kevin Leclerc[1,‡], Lindsey H. Remark[1,2], Malissa Ramsukh[1], Anne Marie Josephson[1,2], Laura Palma[1], Paulo E. L. Parente[1], Margaux Sambon[1], Sooyeon Lee[1,3], Emma Muiños Lopez[1,4], Sophie M. Morgani[1,*] and Philipp Leucht[1,2,*,‡]

ABSTRACT

Periosteal stem and progenitor cells (PSPCs) are major contributors to bone maintenance and repair. Deciphering the molecular mechanisms that regulate their function is crucial for the successful generation and application of future therapeutics. Here, we pinpoint Hox transcription factors as necessary and sufficient for periosteal stem cell function. Hox genes are transcriptionally enriched in periosteal stem cells and their overexpression in more committed progenitors drives reprogramming to a naïve, self-renewing stem cell-like state. Crucially, individual Hox family members are expressed in a location-specific manner and their stem cell-promoting activity is only observed when the Hox gene is matched to the anatomical origin of the PSPC, demonstrating a role for the embryonic Hox code in adult stem cells. Finally, we demonstrate that *Hoxa10* overexpression partially restores the age-related decline in fracture repair. Together, our data highlight the importance of Hox genes as key regulators of PSPC identity in skeletal homeostasis and repair.

KEY WORDS: Skeletal stem cell, Aging, Positional identity, Regeneration, Reprogramming, Stemness

INTRODUCTION

Bone homeostasis and repair are mediated by skeletal stem cells (SSCs) that self-renew and differentiate into the major skeletal/mesenchymal lineages; stromal, osteo, chondro and adipo (Ambrosi et al., 2019; Yue et al., 2016; Zhou et al., 2014). During aging, SSCs are depleted, resulting in weaker bones that are more likely to fracture and that repair less efficiently. Thus, SSCs harbor massive therapeutic potential as a source of differentiated cells to replace those lost and damaged in injury and disease, and are a promising cellular target for rejuvenating the aged skeleton. Nevertheless, while the signals that drive SSC differentiation have been well studied, we know relatively little about the molecular and genetic mechanisms that maintain the stem cell pool. Here, we uncover a previously unreported role for homeobox (Hox) genes in SSC maintenance.

[1]Department of Orthopedic Surgery, NYU Robert I. Grossman School of Medicine, New York, NY 10016, USA. [2]Department of Cell Biology, NYU Robert I. Grossman School of Medicine, New York, NY 10016, USA. [3]Institute of Comparative Molecular Endocrinology, Ulm University, Ulm 89081, Germany. [4]Cell Therapy Area, Clínica Universidad de Navarra, Pamplona 31008, Spain.
*Senior authors

‡Authors for correspondence (philipp.leucht@nyulangone.org; kevin.leclerc@nyulangone.org)

S.M.M., 0000-0002-4290-1080; P.L., 0000-0002-8409-8513

Handling Editor: Patrick Tam
Received 19 October 2022; Accepted 20 February 2023

Hox genes are evolutionarily conserved transcription factors that regulate positional identity and cell fate specification during embryonic development (Deschamps and van Nes, 2005). In mouse and human, there are 39 Hox genes grouped into four clusters, HoxA, HoxB, HoxC and HoxD, in 13 paralogs (Izpisúa-Belmonte et al., 1991; Krumlauf, 1994) that are expressed in a regionally restricted manner. During development, their precise expression pattern establishes the body plan of an organism. At post-natal stages, Hox genes are highly expressed in the stem cells of different species, tissues and organs (Issa et al., 2019; Svingen and Tonissen, 2003; Yoshioka et al., 2021), where they control self-renewal (Magnusson et al., 2007; Yoshioka et al., 2021) and differentiation (Bulajic et al., 2020; Song et al., 2020; Winnik et al., 2009). Therefore, in the adult, the Hox code may also impart positional information that is crucial for tissue homeostasis and regeneration (Pineault et al., 2019; Rux et al., 2016; Yoshioka et al., 2021). In the skeleton, Hox genes are expressed by stem and progenitor cells, and excluded from lineage-restricted cell types (Bradaschia-Correa et al., 2019; Gerber et al., 2018; Leucht et al., 2008; Lin et al., 2021; Pineault et al., 2002; Rux et al., 2016), suggesting that they play a stem cell-specific role. To date, studies have demonstrated that *Hoxa11* is necessary for osteoblast maturation and successful fracture healing of the ulna (Rux et al., 2016; Song et al., 2020), but it is still unknown whether it plays a functional role in the SSC.

Here, we pinpoint Hox genes as being crucial for SSC maintenance. We show that Hox deficiency leads to a decrease in stem cell number and proliferation, and an increase in the propensity of stem cells to undergo spontaneous differentiation toward osteogenic and adipogenic fates. Conversely, an increase in *Hoxa10* expression in skeletal stem and progenitor cultures reduces the differentiation potential of cells, while increasing their self-renewal capacity. During differentiation, SSCs give rise to many fate-restricted progenitors that have limited lineage potential and lifespan (Chan et al., 2015; Debnath et al., 2018). Here, we reveal that Hox overexpression can also drive reprogramming of skeletal progenitors to a more uncommitted stem cell-like state and establish that the reprogramming capacity of individual Hox genes is restricted to cells that are isolated from the specific anatomical region that they are endogenously expressed in. We have previously demonstrated that there is a loss of functional SSCs with age that underpins a decline in the regenerative capacity of the skeleton (Josephson et al., 2019). Here, we show that, during aging, Hox expression is reduced, coincident with the decrease in SSC number, and that *Hoxa10* overexpression partially restores bone regeneration in aged mice. Therefore, reprogramming more prevalent progenitor populations could be an innovative method for rescuing SSC number and a promising strategy for combating bone disorders, such as age-associated bone loss.

Development (2023) 150, dev201391. doi:10.1242/dev.201391

RESULTS

Hox gene expression is enriched in periosteal skeletal stem cells

In various tissues, including the placenta, bone marrow and skeleton, Hox genes are expressed by the stromal cells that mediate tissue repair (Bradaschia-Correa et al., 2019; Hwang et al., 2009; Liedtke et al., 2010; Rux et al., 2016), where they regulate morphogenesis and regeneration (Eckardt et al., 2003; Nogi and Watanabe, 2001; Orii et al., 1999; Thummel et al., 2007). Our RNA-sequencing dataset of whole-bone, hindlimb skeletal elements (Bradaschia-Correa et al., 2019) confirmed that Hox family members are transcriptionally enriched within CD45^{-}Ter119^{-}TIE2^{-}LEPR^{+} skeletal stem and progenitor cells (SSPCs) compared with cells of the bone microenvironment that comprise hematopoietic, endothelial, erythroid (CD45^{+}Ter119^{+}TIE2^{+}LEPR^{variable}) and terminally differentiated skeletal/stromal lineage cells (CD45^{-}Ter119^{-}TIE2^{-}LEPR^{-}), with *Hoxa10* being the most highly expressed (Fig. 1A, Fig. S1).

Skeletal stem and progenitor cells that reside within the periosteum, a thin membrane on the outer surface of the bone, are referred to as periosteal stem and progenitor cells (PSPCs), and are the main contributors to bone repair after injury (Colnot et al., 2012; Duchamp de Lageneste et al., 2018; Ferretti and Mattioli-Belmonte, 2014; Roberts et al., 2015). As such, they represent an ideal cellular therapeutic target for improving fracture healing. Still, the transcriptional signature of PSPCs is distinct from SSPCs found in other regions of the bone (Duchamp de Lageneste et al., 2018) and the role of Hox genes within this population is currently unknown. To examine this, we isolated PSPCs from adult tibiae – the most commonly fractured long bone – via serial collagenase digestions, and performed transcriptional analysis by RNA-sequencing. These data indicated that *Hoxa10* is the most highly expressed family member in the adult tibial periosteum (Fig. 1B, Fig. S2A), which we validated by Nanostring nCounter gene expression analysis (Fig. S2B). PSPCs are a heterogeneous population encompassing naïve periosteal stem cells (PSCs: 6C3^{-}CD90^{-}CD49f^{low}CD51^{low} CD200^{+}CD105^{-}), and more committed periosteal progenitor 1 (PP1: 6C3^{-}CD90^{-}CD49f^{low}CD51^{low}CD200^{-}CD105^{-}) and periosteal progenitor 2 (PP2: 6C3^{-}CD90^{-}CD49f^{low}CD51^{low}CD200^{variable}CD105^{+}) cells (Debnath et al., 2018) (Fig. 1C, Fig. S2C). We found that *Hoxa10* expression was most abundant in PSCs and was significantly reduced as cells progressed along the lineage hierarchy to PP1 and PP2 (Fig. 1D). Correspondingly, in other anatomical locations within the bone, such as the bone marrow, Hox gene expression is specific to progenitor cells and absent in more differentiated lineages (Magnusson et al., 2007; Yoshioka et al., 2021). Here, we have investigated whether this was also the case in the periosteum by studying the early dynamics (the first two hours) of Hox expression during osteogenic and adipogenic differentiation of PSPCs. We observed that *Hoxa10* was rapidly downregulated within 30 min, ahead of other canonical stem cell markers, including *Pdgfra, Twist1* and cyclin D1 (*Ccnd1*) (Fig. 1E,F) (Chan et al., 2015; Duchamp de Lageneste et al., 2018; Morikawa et al., 2009; Pinho et al., 2013). *Hoxa11* and *Hoxc10*, the family members with the second and third highest expression in the tibial periosteum (Fig. S2A,B), were also downregulated at the onset of differentiation (Fig. S2D). Thus, Hox transcription is strongly associated with the most primitive periosteal stem cell state.

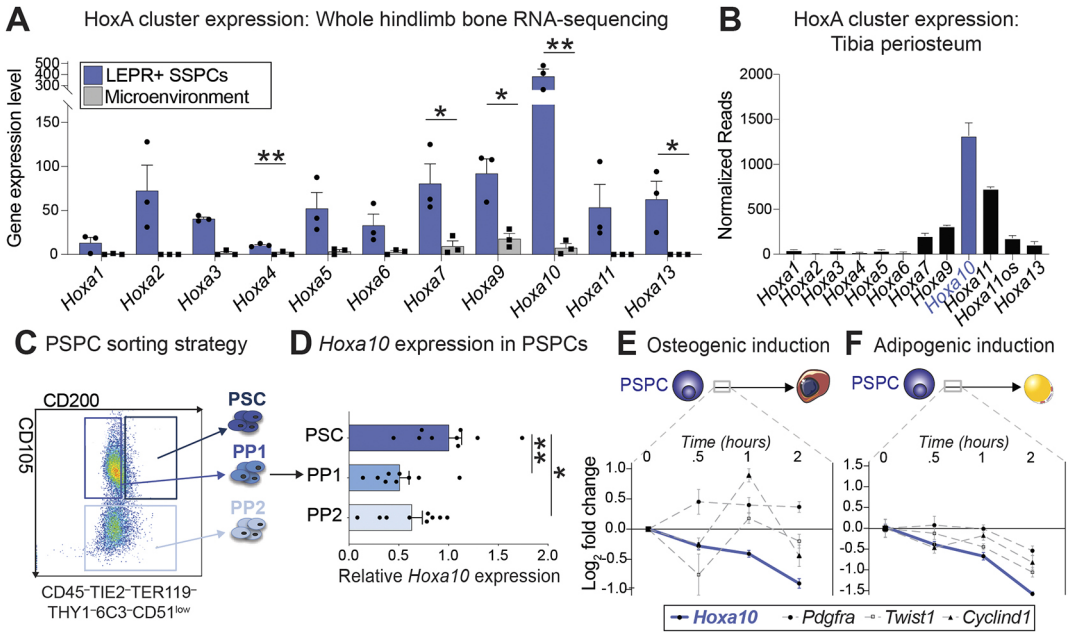

Fig. 1. Hox gene expression is enriched in skeletal stem/progenitor cells. (A) Gene expression pattern for 11 HoxA cluster genes in CD45^{-}TER119^{-}CD31^{-}LEPR^{+} SSPCs or cells of the microenvironment harvested from 12-week-old, freshly isolated tibiae and femurs, as determined by RNA-sequencing (Josephson et al., 2019). HoxA genes are highly enriched in the SSPC population and *Hoxa10*, with the most normalized reads, is the most highly expressed. *n*=3. (B) RNA-sequencing gene expression data of the HoxA cluster derived from 12-week-old tibial periosteal cells. (C) Representative flow cytometry plot of periosteal stem and progenitor cells as defined by Debnath et al. (2018) and strategy for isolating periosteal stem cells (PSC), periosteal progenitor 1 (PP1) cells and periosteal progenitor 2 (PP2) cells. (D) Relative expression of *Hoxa10* in freshly isolated stem and progenitor populations of tibial periosteum as measured by qRT-PCR. *n*=3 mice. (E,F) Gene expression of multiple skeletal stem/progenitor cell-associated genes during a 72 h *in vitro* time course of osteogenic (E) or adipogenic (F) induction of isolated PSCs and PP1 cells, relative to growth media controls. *n*=7 mice. **P*<0.05, ***P*<0.01 (unpaired, two-tailed Student's *t*-test). Each point represents data collected from an individual mouse. Data are mean±s.e.m.

Development (2023) 150, dev201391. doi:10.1242/dev.201391

Hox genes are necessary for periosteal stem cell function

Hox family members regulate stem cell function in multiple tissues and organisms (Bradaschia-Correa et al., 2019; Hwang et al., 2009; Liedtke et al., 2010; Rux et al., 2016). Hox genes are enriched in PSPCs that are responsible for injury repair (Fig. 1). In addition, we observed that Hox genes are downregulated in SSPC/PSPCs during aging (Fig. 2A,B, Fig. S3A), coincident with the loss of SSPC/PSPC number and function, and a decline in the regenerative

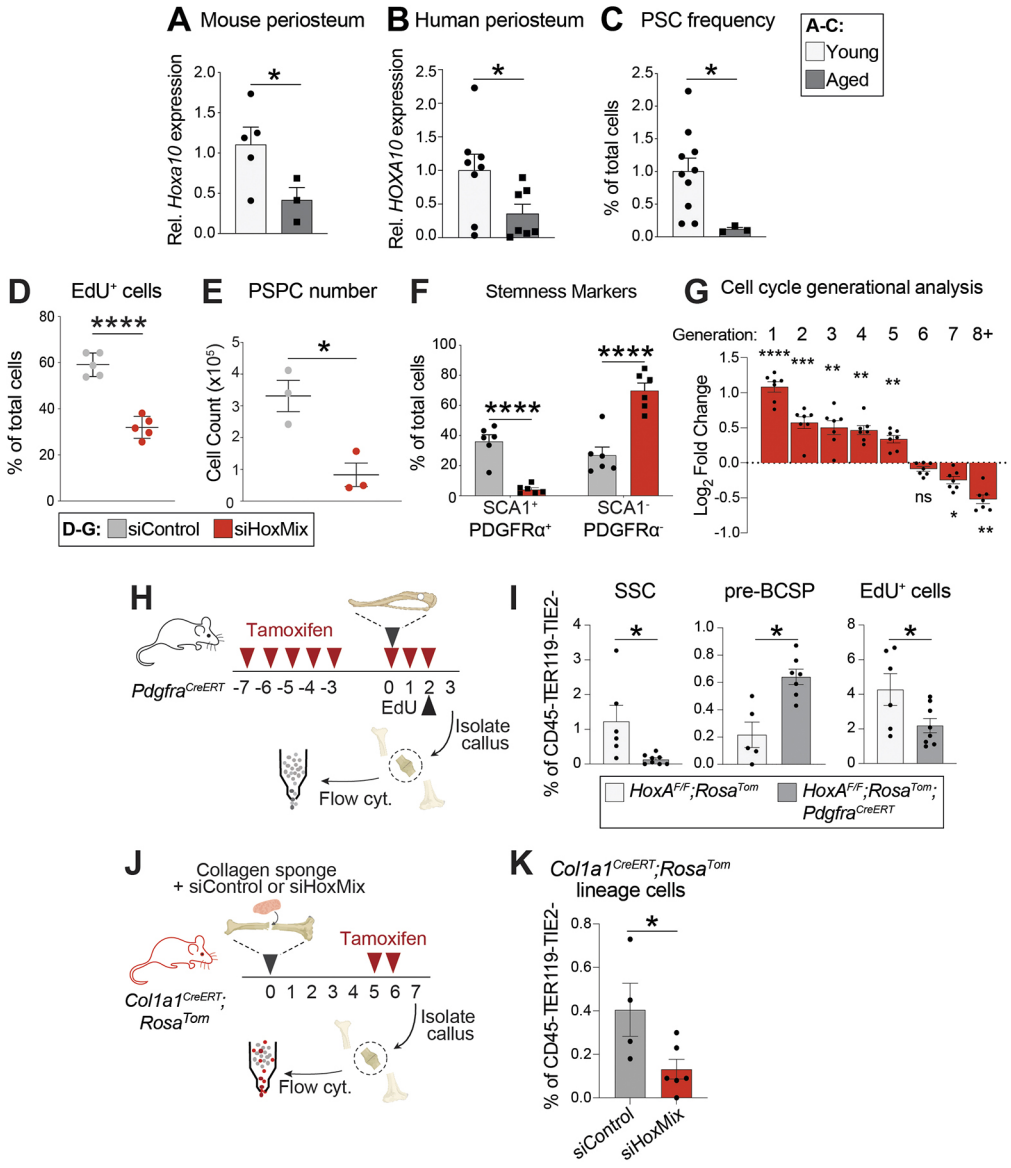

Fig. 2. Loss of Hox genes in stem and progenitor cells triggers a loss of skeletal stem cells and periosteal stemness properties. (A) The relative expression of mouse *Hoxa10* in bone marrow samples harvested from the periosteum of young (3-month-old) and aged (21-month-old) mouse tibiae, as measured by qRT-PCR. *n*=5 (young), *n*=3 (aged). (B) The relative expression of *HOXA10* in bone marrow samples harvested from the fracture sites of young (18-39 years old) and aged (61-86 years old) humans, as measured by qRT-PCR. *n*=8 (young), *n*=7 (aged). (C) When tibial periosteal cells were harvested from young (3-month-old) and aged (21-month-old) mice, flow cytometry revealed the frequency of 6C3$^-$CD90$^-$CD49f^{low}CD51^{low}CD200$^+$CD105$^-$ periosteal stem cells. *n*=10 (young), *n*=3 (aged). (D-G) Simultaneous knockdown of *Hoxa10*, *Hoxa11*, *Hoxd10*, *Hoxd11* and *Hoxc10* (HoxMix) was used to analyze stem cell number (D,E), self-renewal (F) and identity (G) in Hox-deficient tibial PSPCs. (D) PSPCs were pulsed with EdU for 15 h following HoxMix and non-targeting control siRNA knockdown; the number of EdU-positive cells was then measured by flow cytometry. *n*=5. (E) The absolute number of PSPCs after an equal seeding density and 6 days of transfection with either NT control or HoxMix siRNA. *n*=3. (F) After 7 days of control and HoxMix siRNA, PSPCs were analyzed for stemness-associated cell-surface marker expression using flow cytometry. *n*=3 each condition. (G) siControl and siHoxMix tibial PSPCs were also treated with CellTrace and subjected to flow cytometry to categorize cells by generation after 6 days of incubation. The fold change in the percentage of cells treated with siHoxMix in each generation is shown relative to the siControl percentage for each generation. Asterisks indicate statistical significance between siControl and siHoxMix within each generation. *n*=5 (control), *n*=7 (HoxMix). (H) Scheme of tibial defects, tamoxifen dosing protocol (2 mg/day) and EdU administration to test the requirement of HoxA in skeletal stem and progenitor cells. (I) Flow cytometry revealed the percentage of 6C3$^-$CD90$^-$CD51$^+$CD200$^+$CD105$^-$ skeletal stem cells, 6C3$^-$CD90$^-$CD51$^+$CD200$^-$CD105$^-$ pre-bone/chondro/stromal progenitors (pre-BCSPs) and EdU$^+$ proliferative cells in the non-hematopoietic compartment of *Pdgfra*^{CreERT};*HoxA*$^{flox/flox}$ and *HoxA*$^{flox/flox}$ control mice 3 days after tibial defect repair. (J) Experimental plan to test the requirement of multiple posterior Hox genes to generate osteoblasts during bone regeneration of *Col1a1*^{CreERT};*Rosa*^{Tomato} mice. (K) The frequency of Tomato$^+$, osteo-lineage cells in calluses harvested from *Col1a1*^{CreERT};*Rosa*^{Tomato} tibiae undergoing fracture repair at 7 days post-injury, as measured by flow cytometry. *n*=4 mice (control), *n*=6 mice (HoxMix). **P*<0.05, ***P*<0.01, ****P*<0.001, *****P*<0.0001 (unpaired, two-tailed Student's *t*-test). Each point represents data collected from an individual mouse. Data are mean±s.e.m.

Development (2023) 150, dev201391. doi:10.1242/dev.201391

capacity of the skeleton (Fig. 2C) (Josephson et al., 2019). Thus, we hypothesize that Hox genes play a role in regeneration of the skeleton after injury. To investigate this, we assessed the effect of loss of Hox expression on PSPC number, self-renewal and regenerative potential. In knockdown/knockout experiments, the role of individual Hox genes is frequently masked by the functional redundancy of other family members (Carpenter et al., 1993; Gavalas et al., 1998; Mark et al., 1993; McNulty et al., 2005; Rossel and Capecchi, 1999; Rux et al., 2016; Song et al., 2020; Studer et al., 1996). To circumvent these issues, we employed a mix of siRNAs that simultaneously targeted the most highly expressed Hox genes in the tibia (*Hoxa10*, *Hoxa11*, *Hoxd10*, *Hoxd11* and *Hoxc10*), referred to as siHoxMix, which resulted in a significant decrease in their expression (Hoxa10, 85.3%; Hoxa11, 77.6%; Hoxd10, 85.4%; Hoxd11, 53.4%; Hoxc10, 82.8% expression reduction; Fig. S3B).

Self-renewal is a defining property of stem cells and is necessary to maintain the stem cell pool. We observed that treating isolated periosteal cells with siHoxMix caused a decrease in proliferation (Fig. 2D), cell number (Fig. 2E) and the proportion of cells expressing the PSC markers SCA-1 and PDGFRα (Houlihan et al., 2012; Rux et al., 2016) (Fig. 2F). We then quantified self-renewal at a single-cell resolution, using CellTrace, a fluorescent dye that is diluted with each cell division. The amount of dye in each cell after 6 days was measured by flow cytometry and indicates the generation number and cycling rate. Under control conditions, the majority of PSPCs underwent six or more cell divisions and are therefore considered high cycling, a characteristic associated with stemness (Fig. 2G, Fig. S3C,D). Upon Hox knockdown, there was a significant increase in the proportion of cells undergoing five cell divisions or fewer, and, most evidently, in the number of cells that divided only once (Fig. 2G, Fig. S3C). Moreover, sustained knockdown of multiple Hox genes (*Hoxa11*, *Hoxc10* and *Hoxd10*) for 14 days (Fig. S3E) – or the earlier repression of all five Hox genes being studied – led to an upregulation of osteogenic and adipogenic genes at day 14 despite the absence of overt differentiation cues (Fig. S3F), suggesting a progressive exit of cells from the PSC state.

Next, we asked whether this was also the case *in vivo*, employing a $Pdgfra^{CreERT}$ (Wosczyna et al., 2019) mouse line to conditionally delete Hox genes in skeletal stem cells, followed by tibial injury (Lee et al., 2021; Leucht et al., 2007) to stimulate PSPC/SSPC self-renewal (Fig. 2H). To circumvent potential Hox redundancy, we used an allele with *loxP* sites flanking the entire ∼100 kb span of the HoxA cluster (Kmita et al., 2005). Deletion of the HoxA cluster in $Pdgfra^{+}$ PSPCs/SSPCs (Ambrosi et al., 2019; Morikawa et al., 2009; Pinho et al., 2013) (Fig. S3G) led to a reduction of PSCs/SSCs, a concomitant increase in PP1/pre-BCSP (pre-bone, chondro, stromal progenitors) and a significant loss of proliferative capacity compared with $HoxA^{flox/flox}$ control animals (Fig. 2I). Thus, both *in vitro* and *in vivo*, loss of HoxA genes results in a decrease in PSC/SSC self-renewal and/or a loss of stemness, and consequential proportional accumulation of more-committed cell types.

To determine whether a reduction in Hox expression also impaired PSC regenerative function *in vivo*, we fractured the tibiae of young 3-month-old mice and locally delivered siHoxMix on a collagen sponge at the time of injury (we have verified that this delivery method results in widespread transfection; Fig. S3H). We used $Col1a1^{creERT}$;$Rosa^{Tomato}$ mice to label newly formed osteolineage cells and administered tamoxifen at the onset of the differentiation phase of fracture healing (Lee et al., 2021) (5-6 days post-injury, Fig. 2J). At 7 days after injury, fracture sites transduced with siHoxMix displayed a 50% reduction in the proportion of $Tomato^{+}$ cells compared with those transduced with a non-targeting control siRNA (Fig. 2K), demonstrating that the early depletion of Hox genes at the time of PSC self-renewal in response to injury leads to decreased osteolineage output. Together these data demonstrate that Hox genes are necessary to maintain PSPCs in an undifferentiated, self-renewing state, and that decreased Hox expression, as occurs in aging, is sufficient to impede bone regeneration.

Hoxa10 overexpression induces a skeletal stem cell-like state

As Hox knockdown resulted in loss of skeletal stem cell self-renewal, we asked whether, conversely, Hox overexpression promoted stemness and, thus, whether it might represent a strategy for rescuing skeletal stem cell number and function during aging. To this end, we constructed a lentiviral vector harboring the protein-coding sequence of *Hoxa10*, which is the Hox gene most highly expressed in the tibia, along with that of GFP, to fluorescently label infected cells (LV-*Hoxa10*/GFP), and a control vector containing only the GFP-coding sequence (LV-GFP, Fig. S4A). We isolated periosteal cells, infected them with LV-*Hoxa10*/GFP or LV-GFP and confirmed stable *Hoxa10* overexpression (∼25-fold overexpression, Fig. S4B). *Hoxa10* overexpression in periosteal cells increased the proportion of PSPCs (Fig. 3A). Moreover, when exposed to osteo-induction medium for 14 days (Fig. S4C), LV-*Hoxa10*/GFP-transfected cells maintained a significantly greater proportion of PSPCs (Fig. S4D) and expressed significantly lower levels of osteogenic genes [osterix (*Sp7*), osteocalcin (*Bgalp*) and *Runx2*] compared with cells infected with the control virus (Fig. S4E). Therefore, forced expression of *Hoxa10* supports stem cell maintenance.

Hoxa10 overexpression mediates reprogramming of PP1 cells into PSCs

Our observation that *Hoxa10* overexpression increases the number of stem cells in PSPC cultures (Fig. 3A) could be attributed to two mechanisms: an expansion of the stem cell pool through increased self-renewal/proliferation or reprogramming of more committed cells to a stem cell state. First, we examined the possibility that *Hoxa10* overexpression enhances the proliferation of PSPCs, using CellTrace to determine the cycling rate of each stem and progenitor compartment infected with LV-*Hoxa10*/GFP or LV-GFP. *Hoxa10* overexpression did not alter the proliferative rate of any PSPC population (Fig. 3B, Fig. S4F). Therefore, we subsequently investigated the possibility that *Hoxa10* reprograms cells to a more-primitive state by isolating each periosteal stem and progenitor population (PSC, PP1 and PP2) separately, transducing them with LV-*Hoxa10*/GFP or LV-GFP and reassessing the lineage hierarchy after 7 days (Fig. 3C). Control and *Hoxa10*-overexpressing PSCs reconstituted a culture comprising predominantly PP1 cells (Fig. 3D), indicating that PSCs rapidly differentiate into more committed progenitors. This may also reflect the proliferative advantage of PP1 cells (Fig. 3B). However, there was no difference in the distribution of cell populations between LV-*Hoxa10*/GFP and LV-GFP transduced cells (Fig. 3D). When PP1 cells were transduced with LV-*Hoxa10*/GFP or LV-GFP, most cells remained in the PP1 cell state. A small fraction (5%) of LV-GFP-infected PP1 cells gave rise to PSCs. This limited amount of stem cells in the control-infected PP1 cells may reflect a basal level of stochastic sampling of neighboring cellular states, as has been described in many other purified cell populations (Gupta et al., 2011; Wang et al., 2014). Notably, the proportion of PSCs was significantly larger (16%) in LV-*Hoxa10*/GFP-infected PP1 cells at

Development (2023) 150, dev201391. doi:10.1242/dev.201391

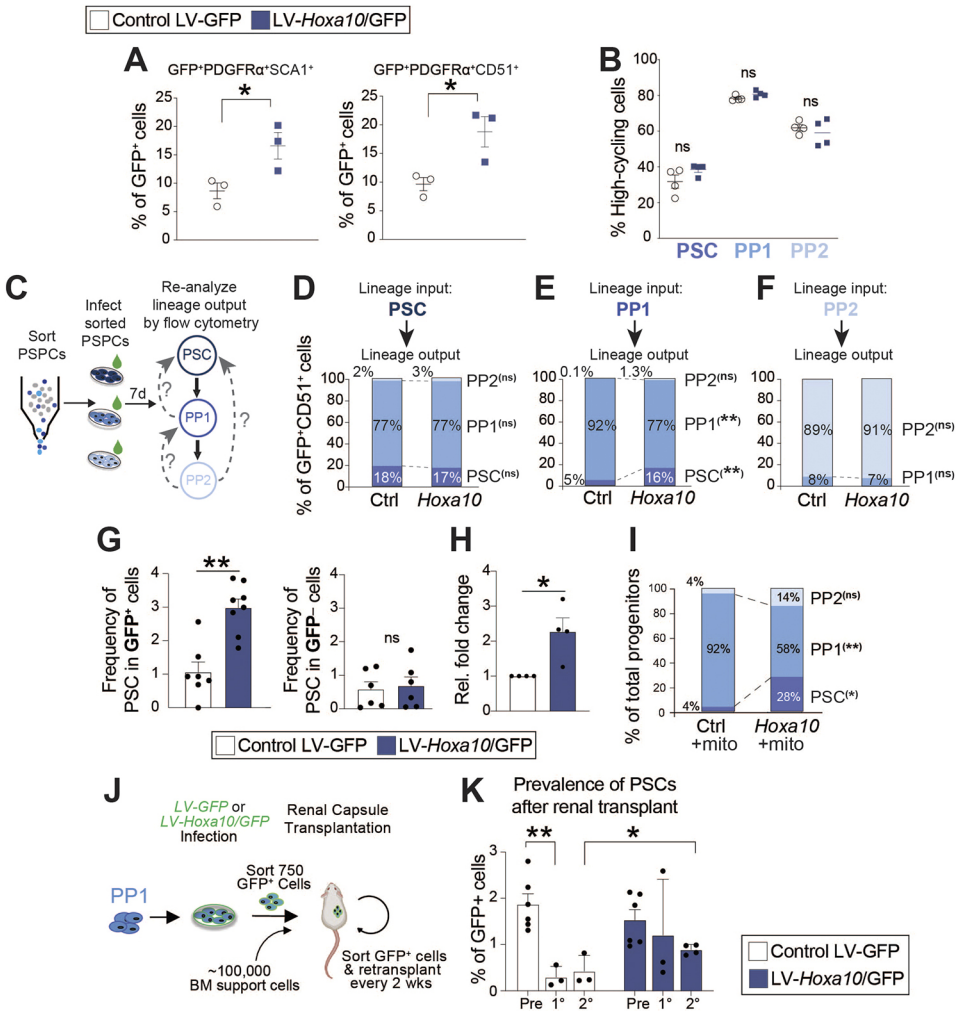

Fig. 3. Hoxa10 overexpression induces a skeletal stem cell-like state. (A) LV-GFP- and LV-*Hoxa10*/GFP-transduced tibial PSPCs were subjected to flow cytometry after a 7-day incubation to analyze the proportion of infected GFP$^+$ cells expressing the skeletal stem cell surface markers PDGFRα/CD51 or PDGFRα/SCA1. *n*=3 mice. (B) LV-GFP- or LV-*Hoxa10*/GFP-infected tibial PSPCs were also treated with Cell Trace and subjected to flow cytometry to categorize cells as high- or low-cycling after 6 days of incubation. Gating strategy is presented in Fig. S4F. *n*=4 for each condition. (C) Experimental plan to test the reprogramming abilities of *Hoxa10*. Tibial PSCs, PP1 and PP2 cells were separately isolated by FACS. Each cell population was infected with LV-GFP or LV-*Hoxa10*/GFP and analyzed by flow cytometry after 7 days of incubation. (D-F) Flow cytometric analysis of the distribution of GFP$^+$ PSCs, PP1 and PP2 cells within the CD51$^+$ stem and progenitor cell compartment 7 days after LV-GFP or LV-*Hoxa10*/GFP infection of PSCs (D), PP1 (E) and PP2 (F) cells. *n*=3 (PSC), *n*=3 (PP1), *n*=5 (PP2). (G) The frequency of PSCs among total cells 7 days after the infection of PP1 cells with LV-GFP or LV-*Hoxa10*/GFP. Infected (GFP$^+$) and uninfected (GFP$^-$) are shown separately. (H) The relative fold change in GFP$^+$ PSCs within the PSPC compartment after transduction of PP1 cells with LV-GFP or LV-*Hoxa10*/GFP. *n*=4 separate experiments. (I) Flow cytometry analysis of the distribution of cells within the PSPC lineage hierarchy after a 7-day treatment of tibial PP1 cells with 10 µg/ml mitomycin C and infection with LV-GFP or LV-*Hoxa10*/GFP. *n*=3. (J) Experimental plan to carry out serial transplants of LV-GFP- or LV-Hoxa10/GFP-treated periosteal PP1 cells under the renal capsule to test self-renewal capacity. (K) PP1 cells were first transduced with either LV-GFP or LV-*Hoxa10*/GFP ,and the prevalence of GFP-labelled PSCs was then assessed by flow cytometry before (Pre) and after each round of transplantation. *n*=6, Pre-LV-GFP and Pre-LV-*Hoxa10*/GFP; *n*=3, 1°-LV-GFP and 1°-LV-*Hoxa10*/GFP; *n*=3, 2°-LV-GFP; *n*=4, 2°-LV-*Hoxa10*/GFP. (D-F,H,I) Complete results and statistics are provided in Table S1. *P<0.05, **P<0.01 (unpaired, two-tailed Student's *t*-test). Each point represents data collected from an individual mouse. Data are mean±s.e.m.

the expense of the PP1 population (Fig. 3E, Fig. S4G). A small fraction of PP2 cells also gave rise to PP1 cells but PP2 cells showed no difference in the relative abundance of the different cell populations when *Hoxa10* was overexpressed (Fig. 3F). Four independent iterations of this experiment confirmed these results, in which *Hoxa10* overexpression in PP1 cells led to a greater than threefold increase in the proportion of PSCs in the progenitor pool (Fig. 3G, Table S1) and an approximately twofold increase in the frequency of PSCs among total *Hoxa10*-overexpressing cells (Fig. 3H); the potential for contaminating PSCs during PP1 isolation was disproven by assessing the post-sorting frequency of PSCs (0%) in the PP1 samples (Fig. S4H). As the Hox and GFP molecules are produced in equimolar amounts from the bicistronic vectors used in these experiments, we used the GFP intensity during flow cytometry analysis to evaluate whether the phenotypic effects of Hox overexpression correlate with overexpression levels. We found that Hoxa10/GFP-expressing converted PSCs had significantly lower GFP expression than the transduced, non-reprogrammed PP1 cells, suggesting that PP1 to PSC conversion preferentially relies upon low overexpression of Hoxa10. PSCs and PP1 cells transduced with the GFP control, on the other hand, displayed no preference for high or low GFP expression (Fig. S4I).

Development (2023) 150, dev201391. doi:10.1242/dev.201391

Although we showed that *Hoxa10* overexpression did not alter PSPC proliferation (Fig. 3B), to unequivocally eliminate the possibility that this result reflected a PSC contamination of the PP1 fraction during cell sorting, and subsequent differential expansion of LV-*Hoxa10*/GFP and LV-GFP transduced cells, we repeated this experiment in the presence of mitomycin C, a potent inhibitor of proliferation. We confirmed an effective inhibition of proliferation in mitomycin C-treated PP1 cells transfected with LV-GFP or LV-*Hoxa10*/GFP (Fig. S5A) and, in the absence of cell division, observed an even greater increase in the proportion of PP1-derived PSCs in *Hoxa10*-overexpressing cells (Fig. 3I). Additionally, neither the lentiviral selection (LV-GFP or LV-*Hoxa10*/GFP) nor the presence of mitomycin C produced a difference in cell death (propidium iodide^{+}) or apoptosis (annexin V^{+}) when total cells, infected cells or individual PSPC compartments were assessed by flow cytometry (Fig. S5B-D). These data demonstrate that the emergence of PSCs from *Hoxa10*/GFP-infected PP1 cells is not due to an expansion of contaminating PSCs or differential cell survival and suggests that progenitors are instead reprogrammed to a less committed state.

To further interrogate the identity of PP1-derived PSC-like cells, we leveraged published single-cell gene expression data (Debnath et al., 2018) to identify novel transcriptional markers of PSCs. We sorted cells *in silico* using defined PSPC cell-surface markers [6C3 (*Enpep*), CD90 (*Thy1*), CD51 (*Itgav*), CD105 (*Eng*) and CD200 (*Cd200*)] and uncovered several factors that were enriched in periosteal stem cells versus PP1 and PP2 cells (*Omd*, *Ucma* and *Frzb*; Fig. S4J). All of these genes were significantly upregulated in PP1 cells transduced with LV-*Hoxa10*/GFP relative to those infected with LV-GFP (Fig. S4K), indicating a shift towards a PSC transcriptome.

Finally, we asked whether PP1-derived PSC-like cells also assume functional properties of PSCs. PSCs are at the top of the PSPC lineage hierarchy and thus possess a greater ability to self-renew than downstream progenitors (Debnath et al., 2018). Accordingly, we asked whether PP1-derived PSC-like cells have a greater self-renewal capacity than PP1 cells. We infected PP1 with LV-*Hoxa10*/GFP or LV-GFP, isolated 300-750 GFP^{+} cells and transplanted them (along with 100,000 bone marrow support cells) for 2 weeks underneath the renal capsule – an environment that is permissive for skeletal stem cell differentiation (Ambrosi et al., 2021; Debnath et al., 2018). GFP^{+} cells were then re-sorted and transplanted for another 2 weeks and the persistence of GFP^{+} PSCs (reprogrammed from PP1 cells) was determined after each transplantation (Fig. 3J). The majority of GFP^{+} PSCs derived from control LV-GFP-infected PP1 cells were lost after only a single round of transplantation, whereas PSCs derived from LV-*Hoxa10*/GFP-infected PP1 cells were maintained after multiple rounds of transplantation, indicating a greater self-renewal capacity (Fig. 3K). Therefore, *Hoxa10* overexpression is sufficient to transcriptionally and functionally reprogram a fraction of PP1 progenitors to a more-primitive PSC state.

The regional specificity of Hox function is maintained in the adult skeleton

During development, individual Hox genes are expressed in different regions of the body. This spatial 'Hox code' is crucial to establish the body plan of the organism (Darbellay et al., 2019; Izpisúa-Belmonte et al., 1991; Papageorgiou, 2012). Hox genes are also expressed in adult skeletal elements and their expression pattern roughly mirrors that during embryogenesis (Fig. 4A) (Ackema and Charité, 2008; Bradaschia-Correa et al., 2019; Leucht et al., 2008; Rux et al., 2016; Rux and Wellik, 2017; Song et al., 2020). Thus, as

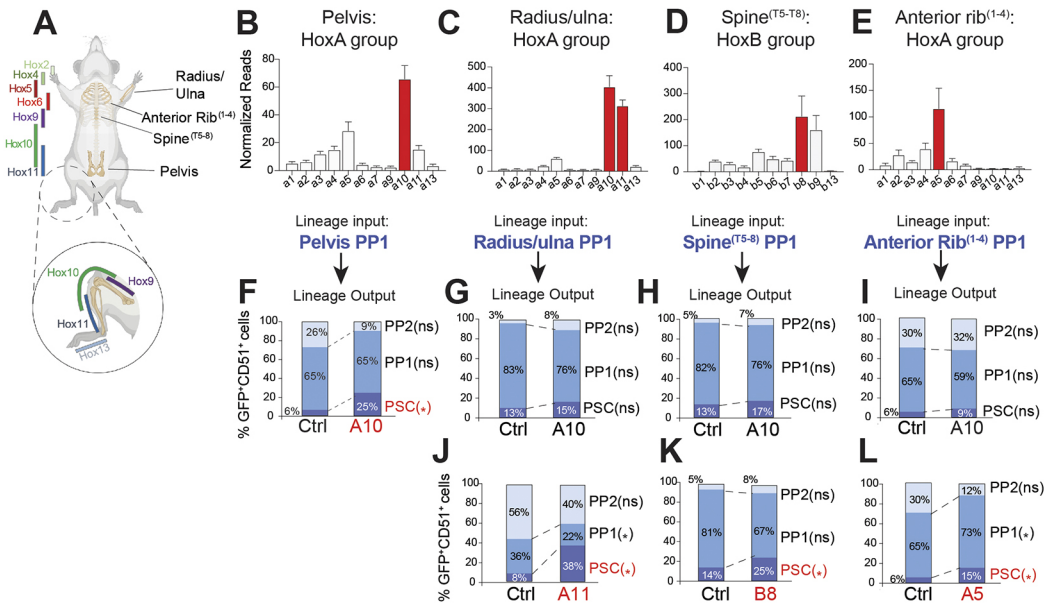

Fig. 4. The regional specificity of Hox function is maintained in the adult skeleton. (A) Diagram of skeletal elements investigated along with the proposed regional restriction Hox expression in adult skeletal tissues (adapted from Rux and Wellik, 2017). (B-E) The expression profile of the Hox cluster containing the highest expressed Hox gene in periosteal cells of the pelvis (B), spine$^{T5\text{-}T8}$ (C), radius/ulna (D) and anterior rib$^{1\text{-}4}$ (E) (highest Hox gene expression is highlighted in red). *n*=4 mice for each skeletal element. Full Hox expression data in Fig. S6. (F-L) The lineage output of stem and progenitors 7 days after infecting PP1 cells derived from the pelvis (F), spine$^{T5\text{-}T8}$ (G,J), radius/ulna (H,K) and anterior rib$^{1\text{-}4}$ (I,L) with LV-*Hoxa10*/GFP (F), LV-*Hoxb8*/GFP (G,J), LV-*Hoxa11*/GFP (H,K) or LV-*Hoxa5*/GFP (I,L), with LV-GFP (Ctrl) and LV-*Hoxa10*/GFP serving as controls. *n*=5, pelvis (control and A10); *n*=4, spine (control and B8); *n*=3, spine (control and A10); *n*=4 and *n*=5, radius/ulna (control and A11, respectively); *n*=5, radius/ulna (control and A10); *n*=9, *n*=8, and *n*=9, anterior rib (control, A5 and A10, respectively). Full lineage output data and statistics are provided in Table S2. n.s., not significant, **P*<0.05 (unpaired, two-tailed Student's *t*-test). Data are mean±s.e.m.

Development (2023) 150, dev201391. doi:10.1242/dev.201391

in development, Hox genes may endow stem cells from different anatomical locations with the specific properties needed to regenerate the tissue in which they reside. Although we previously showed that periosteal cells from skeletal regions with or without Hox expression exhibit functional differences (Bradaschia-Correa et al., 2019; Leucht et al., 2008), the regional specificity of Hox function in the adult has yet to be established. To investigate this, we first precisely defined the adult Hox code, analyzing the expression profile of all 39 Hox genes in periosteal cells from various murine skeletal elements, including the pelvis, thoracic vertebrae 5-8 (spine$^{T5\text{-}8}$), radius/ulna and anterior ribs 1-4. *Hoxa10* was the most highly expressed Hox gene in periosteal cells of the pelvis, radius/ulna and tibia (Figs 1B and 4B,C, Figs S2A,B and S6A), *Hoxb8* was the most highly expressed in the adult spine$^{T5\text{-}8}$ (Fig. 4D, Fig. S6A) and *Hoxa5* was the most highly expressed in the anterior ribs$^{1\text{-}4}$ (Fig. 4E, Fig. S6A).

We then asked whether the stemness-promoting activity of *Hoxa10* is universal or limited to regions where it is most highly expressed (tibia, pelvis and radius/ulna). When periosteal cells from the pelvis, which express high levels of *Hoxa10*, were transduced with LV-*Hoxa10*/GFP, we observed a significant increase in the proportion of PP1-derived PSC-like cells (Fig. 4F, Table S2), as in the tibia (Fig. 3E). In contrast, there was no effect of LV-*Hoxa10*/GFP transduction on periosteal cells from the spine$^{T5\text{-}8}$ or anterior ribs$^{1\text{-}4}$, which express negligible *Hoxa10* (Fig. 4H,I, Table S2), indicating that *Hoxa10* has region-specific function in the adult skeleton. Although we also observed no effect of LV-*Hoxa10*/GFP transduction on periosteal cells from the radius/ulna that highly express both *Hoxa11* and *Hoxa10*, only minor skeletal defects are observed in the radius/ulna of *Hoxa10*$^{-/-}$ mice, whereas *Hoxa11*$^{-/-}$ show severe perturbations (Boulet and Capecchi, 2002; Davis et al., 1995; Favier et al., 1996; Small and Potter, 1993; Wellik and Capecchi, 2003), suggesting that *Hoxa11* plays a key role in that region, despite not being the most highly expressed Hox gene.

Next, we asked whether other Hox family members display the same reprogramming activity as *Hoxa10* in periosteal cells from the skeletal element where they are most abundantly expressed. To this end, we overexpressed *Hoxa11* in radius/ulna, *Hoxb8* in spine$^{T5\text{-}8}$ and *Hoxa5* in anterior rib$^{1\text{-}4}$ periosteal cells. In all cases, we observed a significant increase in the proportion PP1-derived PSC-like cells (Fig. 4J-L, Table S2). As embryonic development progresses anteriorly to posteriorly (and proximal-to-distal in the limb), each Hox gene cluster successively becomes more accessible and expressed, generating a nested pattern where more posterior tissues express a wider set of Hox genes than anterior ones (Tarchini and Duboule, 2006; Papageorgiou, 2012). Thus, posterior tissues may respond to anterior Hox gene expression. To test this, we infected tibial PP1 cells with *Hoxa5* (expressed in the anterior rib$^{1\text{-}4}$) or control lentivirus (Fig. S6B). *Hoxa5* overexpression in posterior progenitor cells did not induce reprogramming (Fig. S6C). Along with *Hoxa10*, *Hoxa11* is also highly expressed in tibia periosteal cells and, when overexpressed, triggered tibia periosteal progenitor cells to revert to a more primitive state (Fig. S6C). Together, these data show that Hox genes promote periosteal stemness in a regionally restricted manner.

Hoxa10 overexpression partially rescues age-related fracture healing deficiency

So far, our data demonstrate that Hox genes are both necessary to maintain a PSC identity and sufficient to induce PSC properties in more-committed progenitors. During aging, Hox genes are downregulated (Fig. 2A,B, Fig. S3A), coincident with a decrease in the number and function of SSPCs/PSPCs, and a consequent decline in the regenerative capacity of the skeleton (Ambrosi et al., 2021; Josephson et al., 2019). Thus, we hypothesized that modulating Hox expression would enhance fracture healing in elderly individuals. To address this hypothesis, we fractured tibiae of young (3-month-old) and middle-aged (13-month-old) wild-type mice, and administered either LV-GFP or LV-*Hoxa10*/GFP, adsorbed into a collagen sponge, to the fracture site at the time of injury (Fig. 5A). Bones were analyzed by µCT at 14 days post-injury, a key stage in the healing process when the injury site progresses to mineralized callus. Bone volume within the callus (BV/TV) is a standardized read-out of bone regeneration. As expected, middle-aged control LV-GFP-transduced tibiae showed a characteristic reduction in callus BV/TV compared with that of young mice (Fig. 5B,C). When middle-aged fracture sites were instead transduced with LV-*Hoxa10*/GFP, we observed a significant increase in BV/TV relative to the middle-aged controls, indicating a partial rescue of fracture healing (Fig. 5B,C). In summary, our data pinpoint Hox genes as essential location-specific regulators of PSC identity, and show that a short-term local increase in their expression is sufficient to augment bone regeneration, highlighting them as promising therapeutic targets for improving the healing of the skeleton in elderly and repair-compromised individuals.

DISCUSSION

Skeletal homeostasis and regeneration rely heavily on stem cells to replenish the tissue lost due to injury or wear and tear. To preserve this capacity, stem cell number has to be constantly maintained by cell division, one of the hallmarks of stemness. Currently, there is a relatively poor understanding of the molecular mechanisms that govern skeletal stem and progenitor cell maintenance over time and lineage progression during bone healing, and this presents one of the major hurdles to advancing cell-based therapies for treatment of bone fractures. The data generated in this study add to the growing appreciation that Hox genes have important functions in the adult skeleton and support a model in which high Hox expression in the uncommitted PSC compartment confers greater self-renewal capacity and moderates lineage progression towards more lineage-restricted cell fates. We also demonstrated that this role of Hox can be exploited to shift periosteal progenitors with limited self-renewal capacity (Debnath et al., 2018) to a more primitive state, thus increasing their functional potential.

Previous reports identified *Hoxa11* as the primary Hox gene that patterns the embryonic tibia and a marker of the adult tibia (Rux et al., 2016; Wellik and Capecchi, 2003). Still, the tibia and fibula are only mildly affected in *Hoxa11*/*Hoxd11* double mutants (Davis et al., 1995; Wellik and Capecchi, 2003), suggesting that other Hox family members are involved in hindlimb development. Both *Hoxa10*$^{-/-}$ and *Hoxd10*$^{-/-}$ mice display defects in the developing hindlimbs, with changes in these structures appearing with greater penetrance in *Hoxa10*$^{-/-}$ mice (Wahba et al., 2001). As we also identified *Hoxa10* as the most highly expressed Hox gene in the adult tibial periosteum (Fig. S2), we decided to investigate its specific role in this skeletal element. Although recent studies demonstrate that *Hoxa11* marks a primitive mesenchymal stem cell (MSC) in the bone marrow and periosteum, and that *Hoxa11* lineage-marked cells are long-term contributors to MSCs throughout life (Pineault et al., 2019; Rux et al., 2016; Song et al., 2020), we show for the first time that Hox genes play a functional role in skeletal stem cell maintenance.

Although loss-of-function studies in other tissues have demonstrated a stem cell maintenance role for Hox genes,

Development (2023) 150, dev201391. doi:10.1242/dev.201391

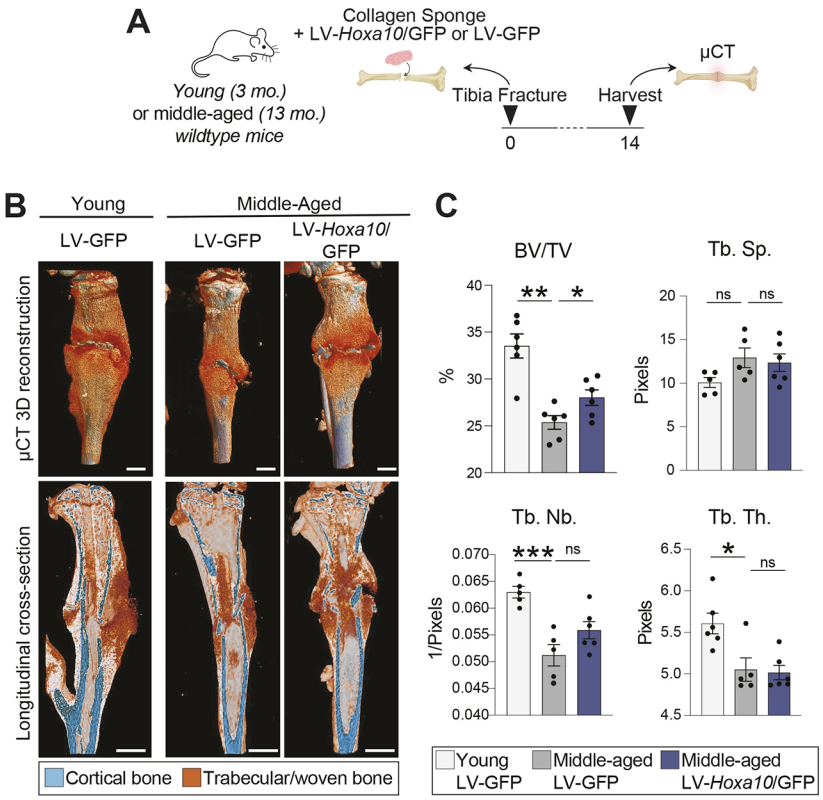

Fig. 5. *In vivo* Hoxa10 overexpression partially rescues age-related fracture-healing deficiency. (A) Experimental plan to test the effect of *Hoxa10* transduction during *in vivo* fracture repair. (B) Representative 3D reconstructions (top) and longitudinal cross-sections (bottom) of young (3-month-old) and middle-aged (13-month-old) tibial fractures transduced with LV-GFP or LV-*Hoxa10*/GFP and imaged by μCT 14 days post-injury. (C) μCT histomorphometry of the calluses of 14-day post-injury tibia fractures in young and middle-aged mice treated with either LV-GFP or LV-*Hoxa10*/GFP. BV/TV, bone volume/total tissue volume; Tb. Sp., trabecular spacing; Tb. Nb., trabecular number; Tb. Th., trabecular thickness. **P*<0.05, ***P*<0.01, ****P*<0.001 (unpaired, two-tailed Student's *t*-test). Each point represents data collected from an individual mouse. Data are mean±s.e.m. Scale bars: 1 mm.

phenotypes have usually been mild (Björnsson et al., 2003; Brun et al., 2004; Iyyanar and Nazarali, 2017; Magli et al., 1997; Owens and Hawley, 2002). Previous studies have also suggested that Hox genes do not play a role in the maintenance of skeletal stem cells. For example, Rux et al. showed that skeletal stem cells harvested from mice in which both alleles of *Hoxd11* and one allele of *Hoxa11* are knocked out display defects in tri-lineage differentiation but do not lose their stemness marker profile or self-renewal capacity (Rux et al., 2016). In addition, after the conditional deletion of *Hoxa11* and *Hoxd11* in 8-week-old forelimbs, skeletal stem cells lacking these genes were still maintained after 10 months (Song et al., 2020). Therefore, individual Hox genes may have distinct functions in the skeletal system. In support of this, previous studies have shown that adjacent Hox genes or Hox genes in the same paralogous group can have opposing functions. For example, in muscle satellite cells, *Hoxa10* promotes proliferation whereas *Hoxa9* and *Hoxc10* disrupt mitosis (Schwörer et al., 2016; Yoshioka et al., 2021). Likewise, *Hoxa5* inhibits endothelial cell differentiation and blocks vascular growth (Rhoads et al., 2005), whereas *Hoxb5* promotes angiogenesis (Winnik et al., 2009). Furthermore, studies focusing on Hox in skeletal tissues typically rely on reducing the expression of one Hox paralogous group (or use single Hox knockout mouse models), and disregard the potential complementation by other highly expressed Hox genes in the cell compartments under study – as observed in the tibial periosteum (Fig. S2A,B). The examination of compound mutants or deficiencies within a Hox cluster or paralogous group may therefore yield more severe phenotypes that can elucidate the role of Hox in adult skeletal cells. In support of this, Hox gain-of-function studies, which can reveal activities masked by functional redundancy, show that Hox genes block differentiation in numerous tissues (Crooks et al., 1999; Fuller et al., 1999; Owens and Hawley, 2002; Schiedlmeier et al., 2003), including *Hoxa10* in hematopoietic and cardiac progenitors (Behrens et al., 2013; Buske et al., 2001; Magnusson et al., 2007; Taghon et al., 2002; Thorsteinsdottir et al., 1997) and *Hoxa2* in murine bone and cartilage development (Creuzet et al., 2002; Kanzler et al., 1998). Here, we have found that the expression of multiple posterior Hox paralogous groups must be decreased to detect a defect in number and function of tibial PSPCs. This functional redundancy may represent a protective evolutionary mechanism to maintain stem cells.

Hox genes have also been shown to regulate osteo-lineage specification. During differentiation of osteoblastic cell lines, *Hoxa10* drives the early expression of osteogenic genes through chromatin remodeling, and the *in vivo* conditional deletion of *Hoxa11* and *Hoxd11* in the *Hoxa11* domain leads to osteogenic differentiation defects (Hassan et al., 2007; Song et al., 2020). In keeping with this, we observed that *Hoxa10* expression decreased within the first few hours of osteogenic and adipogenic differentiation, in line with a stem cell maintenance role, but by around 4 h post-induction, expression returned to the levels seen in non-induced PSPCs (Fig. 1E,F). Thus, Hox genes may play multiple dynamic roles in stem cell maintenance and fate decisions. We demonstrated that *Hoxa10* overexpression leads to a partial restoration of *in vivo* bone regeneration in aged mice (Fig. 5), which could be driven both by an increase in stem cell self-renewal and, at later stages, osteo-lineage commitment. Future studies will precisely dissect the dynamic roles of Hox genes in this process.

Cellular reprogramming is associated with an opening of chromatin (Gaspar-Maia et al., 2011; Ugarte et al., 2015). Several Hox family members (including their *Drosophila* orthologues) function as pioneer factors, demonstrating a preference to bind inaccessible chromatin and, by doing so, increase accessibility (Beh et al., 2016; Bulajic et al., 2020). We also previously showed that Hox-positive periosteal cells have more open chromatin and are more stem-like than periosteal cells derived from Hox-negative

Development (2023) 150, dev201391. doi:10.1242/dev.201391

tissue (Bradaschia-Correa et al., 2019). This, along with the increase in stem cell frequency upon Hox overexpression, led us to postulate that Hox expression drives skeletal progenitors to a more primitive state. We found that overexpression of *Hoxa10* reprogrammed PP1 skeletal progenitors to a stem cell state. Intriguingly, blocking cell division resulted in a massive increase in the efficiency of this process (Fig. 3I). Mitomycin C arrests cells in the G1 phase of the cell cycle (Kang et al., 2001) and multiple studies have connected cell fate decisions to a prolonged G1 (Sela et al., 2012; Tapias et al., 2014). Thus, temporary cell cycle arrest may prolong the permissive window for cell reprogramming to occur. The ability of *Hoxa10* overexpression to reprogram PP1 but not more committed PP2 progenitors is also noteworthy and could represent changes in the epigenetic landscape or a loss of key co-factors at this transition point. Detailed comparisons of the transcriptome and epigenome during progression along this lineage hierarchy will be necessary to gain further insights into the molecular mechanisms of reprogramming.

The continued regional specification of Hox gene expression in adult tissues has been demonstrated by several independent studies, largely by the characterization of cells in culture (Bradaschia-Correa et al., 2019; Chang et al., 2002; Leucht et al., 2008). Here, we corroborate this finding in the periosteal cell compartments of various anatomical regions and, importantly, find that this adult Hox code is functionally relevant to skeletal stem cell regulation. Similarly, in muscle satellite cells derived from the tibialis anterior, ectopic expression of *Hoxa10* was able to rescue proliferation deficiency triggered by the conditional deletion of *Hoxa10* in these cells, but the ectopic expression of *Hoxa5*, *Hoxa9* or *Hoxc10* had no such effect (Yoshioka et al., 2021). Importantly, region-specific Hox function in reprogramming and stem cell maintenance has implications for devising and predicting the engraftment potential of stem cell therapies that target specific segments of the skeleton, or potentially other tissues whose function is controlled by Hox expression profiles.

In contrast to the bone marrow, the periosteum is a relatively understudied tissue. Periosteal progenitor cells play a central role in bone repair and, as such, represent a promising source of cells for tissue engineering approaches. PSPCs also exhibit several characteristics that are advantageous for such strategies, including their high proliferative rate, which is necessary for efficient *in vitro* expansion (Sakaguchi et al., 2005; van Gastel et al., 2012; Yoshimura et al., 2007), and a greater osteogenic capacity than many other mesenchymal stem cell populations both *in vitro* and when transplanted *in vivo* (Roberts et al., 2011, 2015). Looking forward, advances in lineage reprogramming in many tissues have revealed a remarkable flexibility in cell identity (Morris, 2016), and unraveling the mechanisms of reprogramming in skeletal tissues can facilitate the development of cell fate engineering strategies. Further research elucidating the mechanisms by which Hox overexpression increases stem cell potency and how this affects lineage potential can help achieve this therapeutic goal.

MATERIALS AND METHODS

Animals

C57BL/6 mice (8-16 weeks old), were purchased from the Jackson Laboratory and bred in the barrier facility at the New York University School of Medicine. *Pdgfra*$^{CreERT/+}$ knock-in mice were obtained from by the Michael Wosczyna Laboratory at NYU Langone (New York, USA) (Wosczyna et al., 2019). *Col1a1*$^{CreERT/+}$ mice (B6.Cg-Tg(Col1a1-cre/ERT2)1Crm/J) were obtained from the Jackson Laboratory (016241). All mice were bred in the barrier facility at the New York University School of Medicine. To induce recombination in transgenic cre-ERT2 mice, tamoxifen (Sigma-Aldrich) was administered intraperitoneally at 2 mg/day according to the dosing protocol in either Fig. 2H or J. Mice were maintained on a 12-h light/dark cycle with food and water provided *ad libitum*.

Patients and specimens

All experiments involving human subjects were approved by the NYU Robert I. Grossman School of Medicine Institutional Review Board. After informed consent was obtained, bone marrow specimens were obtained during surgery. One cubic centimeter of bone marrow was immediately transferred into a microcentrifuge tube and placed on ice.

Bulk RNA sequencing and Nanostring

FPKM values for each Hox gene were derived from tibial periosteal RNA sequencing data previously published by our group (Bradaschia-Correa et al., 2019; deposited in GEO under accession number GSE173371). Nanostring read counts were determined using the nCounter platform and by generating a custom panel of target-specific oligonucleotide probes (CodeSet) of the 39 murine Hox genes (Table S3). Of the total 78 Hox isoforms produced by the four Hox clusters, only one isoform of *Hoxc4* was not detectable by the custom CodeSet. Five housekeeping genes (*Actb*, *Gusb*, *Pgk1*, *Tbp* and *Tubb*) were used to normalize the read counts.

Periosteal cell isolation

Primary periosteal stem and progenitor cells were obtained from the tibia, pelvis, anterior ribs (1-4), thoracic vertebrae (5-8) of the spine, radius/ulna or parietal/frontal calvaria. After careful dissection from 8- to 16-week-old wild-type (C57BL/6) mice, bones with intact periosteum were submitted to four serial collagenase digestions in 0.2% collagenase type 2 (ThermoFisher Scientific, 17101015) in DMEM (Life Technologies, 11885092) at 37°C for 20 min with gentle rocking. After each of the first three digestions, bones were subjected to light centrifugation (230 ***g***) for 5 min and then transferred to a fresh tube of collagenase. After the last digestion, the bones and cell suspension from the last digestion were centrifuged at 450 ***g*** for 5 min and the pelleted cells were resuspended in growth media (GM): low glucose DMEM (Life Technologies, 11885092), 10% fetal bovine serum (Life Technologies, 10437-028) and 1% penicillin/streptomycin (Life Technologies, 15140122). Selective enrichment of periosteal stem/progenitor cells was confirmed using FACS analysis (Fig. S2C).

Flow cytometry

Cells were trypsinized, resuspended in HBSS (Life Technologies: 14170161), supplemented with 2% fetal bovine serum (Life Technologies, 10437-028), 1% penicillin/streptomycin (Life Technologies: 15140122) and 1% HEPES (Life Technologies, 15630080) (complete HBSS), and stained with 1:300 diluted CD45-PE (Miltenyi Biotec, 130-117-498), TER119-PE (Miltenyi Biotec, 130-117-512, TIE2-PE (ThermoFisher Scientific, 12-5987-82), 6C3-PE (ThermoFisher Scientific, 12-5891-82) and CD90-PE (Invitrogen, MA5-17749), and 1:200 diluted CD51-BV421 (BD Biosciences: 740062), CD105-PE-Cy7 (ThermoFisher Scientific: 25-1051-82) and CD200-BV711 (BD Biosciences: 745548) for 30 min on ice in the dark. Cells were then washed with 1 ml of the complete HBSS solution, centrifuged at 500 ***g*** for 5 min and finally resuspended with complete HBSS for flow cytometry. Cells were sorted on a Sony Biotechnology SY3200 cell sorter into a 50%/50% solution of complete HBSS and fetal bovine serum or analyzed on a Bio-Rad ZE5 Analyzer. Sorting was validated to result in >95% purity of the intended population in post-sort fractions. Beads (eBioscience 01-1111-41) were used to set initial compensation. Fluorescence minus one (FMO) controls were used for additional compensation and to assess background levels for each stain. We excluded doublets and gates were drawn as determined by internal FMO controls to separate positive and negative populations for each cell-surface marker. Mesenchymal cell populations negative for CD45, CD31 and TER119 cell-surface markers were analyzed according to the approach described in Fig. S4G,H.

Development (2023) 150, dev201391. doi:10.1242/dev.201391

Monocortical tibial defects

All procedures followed protocols approved by the NYU Robert I. Grossman School of Medicine Committee on Animal Research. Mice were anesthetized with 1-4% isoflurane inhalation. A 4 mm incision was made over the proximal anteromedial tibia, and the tibial surface was exposed while carefully preserving the periosteum. A 1.0 mm hole was drilled through the anterior cortex with a high-speed dental drill (10,000 rpm). Incisions were closed with 5-0 Vicryl sutures. Before and after surgery, mice received subcutaneous injections of buprenorphine for analgesia and were allowed to ambulate freely. Twenty-four hours before euthanasia mice received 200 µg of EdU to label proliferating cells. Mice were euthanized at indicated days after surgery.

Tibia fractures

Mice were anesthetized using isoflurane inhalation. A 4 mm incision was made over the anteromedial tibial region. The medial and proximal tibia was exposed. Next, a 27G×1-1/4 needle was inserted through the medullary cavity of the tibia to stabilize the ensuing fracture and the tibia was then transected in the mid-diaphysis with small surgical scissors. Hox inhibition was achieved locally by adsorbing 50 nM HoxMix (10 nM each relevant Hox gene) or 50 nM NT Control siRNA into a 2×2×2 mm collagen sponge (DSI Dental Solutions) along with HiPerfect Transfection Reagent (Qiagen) according to the manufacturer's instructions and inserting the sponge under a muscle flap over the tibial fracture site. Transfection efficiency of the collagen sponge delivery method was similarly ascertained with a GFP-tagged siRNA (MISSION siRNA Fluorescent Universal Negative Control; Millipore Sigma, SIC003).

Conversely, to overexpress *Hoxa10*, either LV-GFP or LV-*Hoxa10*/GFP was combined with *pLenti-rtTA* (all lentiviral constructs at a M.O.I. of 150) and 2.5 µg/ml polybrene. The mixture was then adsorbed into a 2×2×2 mm collagen sponge (DSI Dental Solutions) that was then inserted under a muscle flap over the tibial fracture site.

For all experiments, incisions were closed with 5-0 Vicryl sutures. Before and after surgery, mice received subcutaneous injections of buprenorphine for analgesia and were allowed to ambulate freely.

µCT analyses

Tibias were scanned using a high-resolution SkyScan µCT system (SkyScan 1172, Bruker). Images were acquired at 9 µm isotropic resolution using a 10 MP digital detector, 10 W energy (100 kV and 100A) and a 0.5 mm aluminum filter with a 9.7 µm image voxel size. A fixed global threshold method was used based on the manufacturer's recommendations and preliminary studies showed that mineral variation between groups was not high enough to warrant adaptive thresholding. The samples were oriented and the volume of interest (VOI) defined with the CTAn software (Bruker). The VOI was contoured manually to capture the entire callus region. The parameters selected to show variations between groups were total bone volume (BV), total tissue volume (TV), relative mineralized volume fraction (BV/TV), trabecular number (Tb.N), trabecular thickness (Tb.Th) and trabecular spacing (Tb.Sp) following the guidelines described by Bouxsein et al. (2010).

In vitro differentiation

5×10^4 PSPCs or sorted PP1 cells were seeded onto individual wells of 24-well plates [wells were first coated with a 1:100 dilution of fibronectin (Sigma: F0895) in PBS for 60 min] in GM and allowed to attach overnight. The next day, cells were stimulated with osteogenic media (OM) [DMEM, 10% FBS, 100 µg/ml ascorbic acid, 10 mM β-glycerophosphate and 1% penicillin/streptomycin]. Media were replenished every 2-3 days. For adipogenic differentiation, the cells were induced the next day using the MSC Adipogenic BulletKit (Lonza) induction media.

RNA interference

Primary PSPCs were transfected with a commercially available GeneSolution siRNAs targeting *Hoxa10* (CACCACAATTCTCCC-TATTTA; Qiagen, SI01068753), *Hoxd10* (CCGAACAGATCTTGTC-GAATA; Qiagen, SI00206542), *Hoxc10* (TTCGAGGATGCTTCCACC TAA; Qiagen, SI01069306), *Hoxa11* (CACCACTGATCTGCACC-CAAA; Qiagen, SI01068788) and *Hoxd11* (CCCGTCGGACTTCGC-CAGCAA; Qiagen, SI01069558). AllStars Negative Control siRNA (Qiagen, 1027281) was used as a non-targeting control. Each component siRNA of HoxMix was delivered at 5 nM, yielding a total HoxMix concentration of 25 nM; non-targeting control siRNA was delivered at 25 nM. HiPerfect Transfection Reagent (Qiagen) was used as a transfection reagent according to the manufacturer's instructions. Transfection was carried out at the moment of seeding onto multiwell plates before the cells fully attached to the plates (fast-forward transfection). The seeded cells were treated with siRNAs every 3 to 4 days, and samples were assayed by qRT-PCR or flow cytometry after 2-14 days of knockdown.

Proliferation assay

5×10^4 PSPCs were seeded onto wells of 24-well plates in GM and simultaneously administered either HoxMix or nontargeting siRNAs. After 24 h, the cells were incubated with 10 µM EdU at 37°C for 15 h, washed with PBS and then trypsinized. The Click-iT Plus EdU Alexa Fluor 488 Flow Cytometry Kit (ThermoFisher Scientific, C10632) was used to fix, permeabilize and label EdU-incorporated cells with a Click-iT reaction according to the manufacturer's instructions before subjecting the cells to flow cytometry analysis thereafter.

Cell-cycle analysis

CellTrace Far Red Cell Proliferation Kit (ThermoFisher Scientific, C34564) was used according to the manufacturer's instructions. In the RNA interference experiments, PSPCs isolated from C57BL/6 wild-type mice were first expanded *in vitro*, and 5×10^4 cells were then seeded onto individual wells of a 24-well plate with HoxMix or nontargeting siRNA. 24 h later, the cells from each well were trypsinized, incubated with CellTrace for 1 h at 37°C on day 0, then replated and cultured for 6 days. On day 6, cells were trypsinized and stained for PDGFRα (Invitrogen, 25-1401-82). A separate batch of cells was also trypsinized and incubated with CellTrace for 1 h at 37°C on day 6 to serve as a positive control.

For the overexpression experiments, PSCs, PP1 and PP2 cells were sorted from *in vitro*-expanded PSPCs. 3×10^4 cells were incubated with either LV-GFP or LV-*Hoxa10*/GFP in individual wells of a 24-well plate. After 24 h, the procedure was then continued as described above. Cells in this case were stained with the lineage cell surface markers previously described (Debnath et al., 2018). Cells were then analyzed on a BD Biosciences LSRII UV cell analyzer for dye dilution and surface marker profile.

RNA isolation and quantitative real-time PCR

RNA was either isolated from cells immediately after periosteal isolation and FACS to observe *in vivo* gene expression or from cells expanded *in vitro*. The RNeasy Plus Kit (Qiagen, 74134) was used to isolate RNA and remove genomic DNA. RNA was then reverse-transcribed with the iScript cDNA Synthesis Kit (Bio-Rad, 170-8891). Quantitative real-time PCR was carried out using the Applied Biosystems QuantStudio3 system and RT^2 SYBR Green ROX PCR Master Mix (Qiagen, 330523). Specific primers were designed using Harvard PrimerBank (http://pga.mgh.harvard.edu/primerbank/) (Table S4). Results are presented as $2^{-\Delta\Delta Ct}$ values normalized to the expression of 18s. Mean and s.e.m. were calculated in GraphPad Prism 7 software.

Viral generation and transduction

Lentiviral DNA containing either a *Hoxa10* CDS expression construct or a control construct lacking *Hoxa10* CDS was generated at Genewiz using the Tet-ON system. In addition to the *Hoxa10* sequence, the lentiviral vector used (*ptetO*) also include EGFP, luciferase and puromycin cloned downstream of the active CMV promoter. 2A peptide sequences are also included between each element (*ptetO-Hoxa10-T2A-EGFP-P2A-Luciferase-T2A-Puromycin*; LV-*Hoxa10*/GFP and *ptetO-EGFP-P2A-Luciferase-T2A-Puromycin*; LV-GFP) in order to produce multi-cistronic, equimolar expression of all four genes. EGFP was used to track the cells that have been infected in culture. Identical methods were used to generate

lentiviral sequences containing *Hoxa11*, *Hoxb8* and *Hoxa5*. *pLenti-rtTA3* (Addgene #26429), *pRSV-Rev* (Addgene #12259), *pMD2.G* (Addgene #12259), and *pMDLg/pRRE* (Addgene #12251) plasmids were purchased and lentivirus was generated in the Lenti-X 293T Cell Line (TakaraBio, 632180), purified with a Lenti-X Maxi Purification Kit (TakaraBio, 631234) and titered with a Lenti-X qRT-PCR Titration Kit (TakaraBio, 631235).

3×10^4 sorted PSCs, PP1, PP2 or *in vitro*-expanded PSPCs were seeded onto individual wells of 24-well plates [wells were first coated with a 1:100 dilution of fibronectin (Sigma, F0895) in PBS for 60 min] using GM made with 10% heat-inactivated fetal bovine serum and 1% penicillin/streptomycin. The cells were immediately transduced with *pLenti-rtTA* and LV-GFP, LV-*Hoxa10*/GFP, LV-*Hoxa11*/GFP, LV-*Hoxb8*/GFP or LV-*Hoxa5*/GFP at a M.O.I. of 75. The transduction efficiency was aided by the addition of 2.5 µg/ml polybrene (Sigma) and the cells were treated with 10 µg/ml doxycycline to activate expression downstream of the tetO promoter sequences. GM with 10 µg/ml doxycycline was used to replace the media every 2-3 days.

Identification of PSC markers from dataset

The periosteal scRNA-seq dataset is from a publicly available adult mouse femoral periosteum study (Debnath et al., 2018). We obtained the raw count matrix from the GEO deposit GSE106236 and annotated cells based on high expression levels of the genes associated with the cell-surface markers used for flow cytometry [6C3 (*Enpep*), CD90 (*Thy1*), CD51 (*Itgav*), CD105 (*Eng*) and CD200 (*Cd200*)]. The PSC, PP1 and PP2 cells in the count matrix were then sorted *in silico* according to a previously described gating strategy presented in the results (Debnath et al., 2018); genes with a high fold change between PSCs and PP1/PP2 cells were used to identify potential PSC markers.

Renal capsule transplants

A model of mesenchymal stem cell differentiation was used to compare the regenerative potential of PSPCs. 12- to 15-week-old syngeneic C57BL/6 mice were used as hosts for the renal capsule transplantation assay. An incision was made on the dorsal skin surface, followed by an incision through the peritoneum, and the kidneys were identified and then exteriorized. An incision in the renal capsule was made using a 27-gauge needle. Tibial bone marrow (2 µl, containing ∼100,000 cells) from 12-week-old C57BL/6 mice was used to resuspend 750 transduced (GFP^+) PP1 cells. The mixture was then left exposed to open air for 1-2 min to allow a limited amount of coagulation to take place and subsequently grafted beneath the capsule. The kidney was placed back into its anatomical location and the peritoneum was closed using a Vicryl suture, followed by skin closure with a 6-0 Vicryl suture. Mice had *ad libitum* access to food and water (with dissolved 0.4 mg/ml doxycycline and 5% sucrose) and received subcutaneous buprenorphine for analgesia. Mice were euthanized 14 days post-surgery, and the renal grafts were harvested, digested in 0.2% collagenase type 2 (ThermoFisher Scientific) in DMEM at 37°C for 1 h, stained with antibodies and subjected to FACS. The GFP^+ cells were collected and reused for the subsequent renal grafts.

Acknowledgements

We thank Gozde (Gina) Yildirim, MS (NYU College of Dentistry) for assistance with the µCT imaging [funded by the National Institutes of Health (S10OD010751)] and the Preclinical Imaging Laboratory [a shared resource partially supported by a Laura and Isaac Perlmutter Cancer Center support grant (NIH/NCI 5P30CA016087) and by a NIBIB Biomedical Technology Resource Center Grant (NIH P41 EB017183)]. Cell sorting/flow cytometry technologies were provided by NYU Langone's Cytometry and Cell Sorting Laboratory, which is supported in part by grant P30CA016087 from the National Institutes of Health/National Cancer Institute. RNAseq/ATACseq was performed in the NYU Langone's Genome Technology Center, partially supported by the Cancer Center Support Grant P30CA016087 at the Laura and Isaac Perlmutter Cancer Center. We thank the Genotyping Core Laboratory at NYU Langone for their assistance.

Competing interests

The authors declare no competing or financial interests.

Author contributions

Conceptualization: K.L., S.M.M., P.L.; Methodology: K.L., M.R.; Formal analysis: K.L., L.H.R., M.R., S.L., S.M.M., P.L.; Investigation: K.L., L.H.R., M.R., A.M.J., L.P., P.E.L.P., M.S., S.L., E.M.L.; Data curation: K.L.; Writing - original draft: K.L., S.M.M., P.L.; Writing - review & editing: S.M., P.L.; Supervision: S.M., P.L.; Funding acquisition: P.L.

Funding

This work was supported by the National Institute on Aging (R01AG056169 to P.L.), by the National Institutes of Health/National Institute of Arthritis and Musculoskeletal and Skin (K08AR069099 to P.L.) and by a Career Development Award from the Musculoskeletal Transplant Foundation (P.L.). P.L. is also supported a gift from the Patricia and Frank Zarb Family. K.L. is supported by the National Center for Advancing Translational Sciences (NCATS), National Institutes of Health, through grant award number TL1TR001447. S.M.M. is a New York Stem Cell Foundation – Druckenmiller Fellow. Deposited in PMC for release after 12 months.

Data availability

All relevant data can be found within the article and its supplementary information.

References

Ackema, K. B. and Charité, J. (2008). Mesenchymal stem cells from different organs are characterized by distinct topographic Hox codes. *Stem Cells Dev.* **17**, 979-992. doi:10.1089/scd.2007.0220

Ambrosi, T. H., Longaker, M. T. and Chan, C. K. F. (2019). A revised perspective of skeletal stem cell biology. *Front. Cell Dev. Biol.* **7**, 189. doi:10.3389/fcell.2019.00189

Ambrosi, T. H., Marecic, O., McArdle, A., Sinha, R., Gulati, G. S., Tong, X., Wang, Y., Steininger, H. M., Hoover, M. Y., Koepke, L. S. et al. (2021). Aged skeletal stem cells generate an inflammatory degenerative niche. *Nature* **597**, 256-262. doi:10.1038/s41586-021-03795-7

Beh, C. Y., El-Sharnouby, S., Chatzipli, A., Russell, S., Choo, S. W. and White, R. (2016). Roles of cofactors and chromatin accessibility in Hox protein target specificity. *Epigenet. Chromatin* **9**, 1. doi:10.1186/s13072-015-0049-x

Behrens, A. N., Iacovino, M., Lohr, J. L., Ren, Y., Zierold, C., Harvey, R. P., Kyba, M., Garry, D. J. and Martin, C. M. (2013). Nkx2-5 mediates differential cardiac differentiation through interaction with Hoxa10. *Stem Cells Dev.* **22**, 2211-2220. doi:10.1089/scd.2012.0611

Björnsson, J. M., Larsson, N., Brun, A. C., Magnusson, M., Andersson, E., Lundström, P., Larsson, J., Repetowska, E., Ehinger, M., Humphries, R. K. et al. (2003). Reduced proliferative capacity of hematopoietic stem cells deficient in Hoxb3 and Hoxb4. *Mol. Cell. Biol.* **23**, 3872-3883. doi:10.1128/MCB.23.11.3872-3883.2003

Boulet, A. M. and Capecchi, M. R. (2002). Duplication of the Hoxd11 gene causes alterations in the axial and appendicular skeleton of the mouse. *Dev. Biol.* **249**, 96-107. doi:10.1006/dbio.2002.0755

Bouxsein, M. L., Boyd, S. K., Christiansen, B. A., Guldberg, R. E., Jepsen, K. J. and Müller, R. (2010). Guidelines for assessment of bone microstructure in rodents using micro-computed tomography. *J. Bone Miner. Res.* **25**, 1468-1486. doi:10.1002/jbmr.141

Bradaschia-Correa, V., Leclerc, K., Josephson, A. M., Lee, S., Palma, L., Litwa, H. P., Neibart, S. S., Huo, J. C. and Leucht, P. (2019). Hox gene expression determines cell fate of adult periosteal stem/progenitor cells. *Sci. Rep.* **9**, 5043. doi:10.1038/s41598-019-41639-7

Brun, A. C. M., Björnsson, J. M., Magnusson, M., Larsson, N., Leveén, P., Ehinger, M., Nilsson, E. and Karlsson, S. (2004). Hoxb4-deficient mice undergo normal hematopoietic development but exhibit a mild proliferation defect in hematopoietic stem cells. *Blood* **103**, 4126-4133. doi:10.1182/blood-2003-10-3557

Bulajic, M., Srivastava, D., Dasen, J. S., Wichterle, H., Mahony, S. and Mazzoni, E. O. (2020). Differential abilities to engage inaccessible chromatin diversify vertebrate Hox binding patterns. *Development* **147**, dev194761. doi:10.1242/dev.194761

Buske, C., Feuring-Buske, M., Antonchuk, J., Rosten, P., Hogge, D. E., Eaves, C. J. and Humphries, R. K. (2001). Overexpression of HOXA10 perturbs human lymphomyelopoiesis in vitro and in vivo. *Blood* **97**, 2286-2292. doi:10.1182/blood.V97.8.2286

Carpenter, E. M., Goddard, J. M., Chisaka, O., Manley, N. R. and Capecchi, M. R. (1993). Loss of Hox-A1 (Hox-1.6) function results in the reorganization of the murine hindbrain. *Development* **118**, 1063-1075. doi:10.1242/dev.118.4.1063

Chan, C. K. F., Seo, E. Y., Chen, J. Y., Lo, D., McArdle, A., Sinha, R., Tevlin, R., Seita, J., Vincent-Tompkins, J., Wearda, T. et al. (2015). Identification and specification of the mouse skeletal stem cell. *Cell* **160**, 285-298. doi:10.1016/j.cell.2014.12.002

Chang, H. Y., Chi, J.-T., Dudoit, S., Bondre, C., van de Rijn, M., Botstein, D. and Brown, P. O. (2002). Diversity, topographic differentiation, and positional memory in human fibroblasts. *Proc. Natl. Acad. Sci. USA* **99**, 12877-12882. doi:10.1073/pnas.162488599

Colnot, C., Zhang, X. and Knothe Tate, M. L. (2012). Current insights on the regenerative potential of the periosteum: molecular, cellular, and endogenous engineering approaches. *J. Orthop. Res.* **30**, 1869-1878. doi:10.1002/jor.22181
Creuzet, S., Couly, G., Vincent, C. and Le Douarin, N. M. (2002). Negative effect of Hox gene expression on the development of the neural crest-derived facial skeleton. *Development* **129**, 4301-4313. doi:10.1242/dev.129.18.4301
Crooks, G. M., Fuller, J., Petersen, D., Izadi, P., Malik, P., Pattengale, P. K., Kohn, D. B. and Gasson, J. C. (1999). Constitutive HOXA5 expression inhibits erythropoiesis and increases myelopoiesis from human hematopoietic progenitors. *Blood* **94**, 519-528. doi:10.1182/blood.V94.2.519.414k20_519_528
Darbellay, F., Bochaton, C., Lopez-Delisle, L., Mascrez, B., Tschopp, P., Delpretti, S., Zakany, J. and Duboule, D. (2019). The constrained architecture of mammalian Hox gene clusters. *Proc. Natl. Acad. Sci. USA* **116**, 13424-13433. doi:10.1073/pnas.1904602116
Davis, A. P., Witte, D. P., Hsieh-Li, H. M., Potter, S. S. and Capecchi, M. R. (1995). Absence of radius and ulna in mice lacking hoxa-11 and hoxd-11. *Nature* **375**, 791-795. doi:10.1038/375791a0
Debnath, S., Yallowitz, A. R., McCormick, J., Lalani, S., Zhang, T., Xu, R., Li, N., Liu, Y., Yang, Y. S., Eiseman, M. et al. (2018). Discovery of a periosteal stem cell mediating intramembranous bone formation. *Nature* **562**, 133-139. doi:10.1038/s41586-018-0554-8
Deschamps, J. and van Nes, J. (2005). Developmental regulation of the Hox genes during axial morphogenesis in the mouse. *Development* **132**, 2931-2942. doi:10.1242/dev.01897
Duchamp de Lageneste, O., Julien, A., Abou-Khalil, R., Frangi, G., Carvalho, C., Cagnard, N., Cordier, C., Conway, S. J. and Colnot, C. (2018). Periosteum contains skeletal stem cells with high bone regenerative potential controlled by Periostin. *Nat. Commun.* **9**, 773. doi:10.1038/s41467-018-03124-z
Eckardt, H., Bundgaard, K. G., Christensen, K. S., Lind, M., Hansen, E. S. and Hvid, I. (2003). Effects of locally applied vascular endothelial growth factor (VEGF) and VEGF-inhibitor to the rabbit tibia during distraction osteogenesis. *J. Orthopaedic Res.* **21**, 335-340. doi:10.1016/S0736-0266(02)00159-6
Favier, B., Rijli, F. M., Fromental-Ramain, C., Fraulob, V., Chambon, P. and Dollé, P. (1996). Functional cooperation between the non-paralogous genes Hoxa-10 and Hoxd-11 in the developing forelimb and axial skeleton. *Development* **122**, 449-460. doi:10.1242/dev.122.2.449
Ferretti, C. and Mattioli-Belmonte, M. (2014). Periosteum derived stem cells for regenerative medicine proposals: Boosting current knowledge. *World J. Stem Cells* **6**, 266-277. doi:10.4252/wjsc.v6.i3.266
Fuller, J. F., McAdara, J., Yaron, Y., Sakaguchi, M., Fraser, J. K. and Gasson, J. C. (1999). Characterization of HOX gene expression during myelopoiesis: role of HOX A5 in lineage commitment and maturation. *Blood* **93**, 3391-3400. doi:10.1182/blood.V93.10.3391.410k26_3391_3400
Gaspar-Maia, A., Alajem, A., Meshorer, E. and Ramalho-Santos, M. (2011). Open chromatin in pluripotency and reprogramming. *Nat. Rev. Mol. Cell Biol.* **12**, 36-47. doi:10.1038/nrm3036
Gavalas, A., Studer, M., Lumsden, A., Rijli, F. M., Krumlauf, R. and Chambon, P. (1998). Hoxa1 and Hoxb1 synergize in patterning the hindbrain, cranial nerves and second pharyngeal arch. *Development* **125**, 1123-1136. doi:10.1242/dev.125.6.1123
Gerber, T., Murawala, P., Knapp, D., Masselink, W., Schuez, M., Hermann, S., Gac-Santel, M., Nowoshilow, S., Kageyama, J., Khattak, S. et al. (2018). Single-cell analysis uncovers convergence of cell identities during axolotl limb regeneration. *Science* **362**, eaaq0681. doi:10.1126/science.aaq0681
Gupta, P. B., Fillmore, C. M., Jiang, G., Shapira, S. D., Tao, K., Kuperwasser, C. and Lander, E. S. (2011). Stochastic state transitions give rise to phenotypic equilibrium in populations of cancer cells. *Cell* **146**, 633-644. doi:10.1016/j.cell.2011.07.026
Hassan, M. Q., Tare, R., Lee, S. H., Mandeville, M., Weiner, B., Montecino, M., van Wijnen, A. J., Stein, J. L., Stein, G. S. and Lian, J. B. (2007). HOXA10 controls osteoblastogenesis by directly activating bone regulatory and phenotypic genes. *Mol. Cell. Biol.* **27**, 3337-3352. doi:10.1128/MCB.01544-06
Houlihan, D. D., Mabuchi, Y., Morikawa, S., Niibe, K., Araki, D., Suzuki, S., Okano, H. and Matsuzaki, Y. (2012). Isolation of mouse mesenchymal stem cells on the basis of expression of Sca-1 and PDGFR-α. *Nat. Protoc.* **7**, 2103-2111. doi:10.1038/nprot.2012.125
Hwang, J. H., Seok, O. S., Song, H.-R., Jo, J. Y. and Lee, J. K. (2009). HOXC10 as a potential marker for discriminating between amnion- and decidua-derived mesenchymal stem cells. *Cloning Stem Cells* **11**, 269-279. doi:10.1089/clo.2008.0068
Issa, A. R., Picao-Osorio, J., Rito, N., Chiappe, M. E. and Alonso, C. R. (2019). A single microRNA-Hox gene module controls equivalent movements in biomechanically distinct forms of Drosophila. *Curr. Biol.* **29**, 2665-2675.e2664. doi:10.1016/j.cub.2019.06.082
Iyyanar, P. P. R. and Nazarali, A. J. (2017). Hoxa2 inhibits bone morphogenetic protein signaling during osteogenic differentiation of the palatal mesenchyme. *Front. Physiol.* **8**, 929. doi:10.3389/fphys.2017.00929
Izpisúa-Belmonte, J. C., Falkenstein, H., Dollé, P., Renucci, A. and Duboule, D. (1991). Murine genes related to the Drosophila AbdB homeotic genes are sequentially expressed during development of the posterior part of the body. *EMBO J.* **10**, 2279-2289. doi:10.1002/j.1460-2075.1991.tb07764.x
Josephson, A. M., Bradaschia-Correa, V., Lee, S., Leclerc, K., Patel, K. S., Muinos Lopez, E., Litwa, H. P., Neibart, S. S., Kadiyala, M., Wong, M. Z. et al. (2019). Age-related inflammation triggers skeletal stem/progenitor cell dysfunction. *Proc. Natl. Acad. Sci. USA* **116**, 6995-7004. doi:10.1073/pnas.1810692116
Kang, S. G., Chung, H., Yoo, Y. D., Lee, J. G., Choi, Y. I. and Yu, Y. S. (2001). Mechanism of growth inhibitory effect of Mitomycin-C on cultured human retinal pigment epithelial cells: apoptosis and cell cycle arrest. *Curr. Eye Res.* **22**, 174-181. doi:10.1076/ceyr.22.3.174.5513
Kanzler, B., Kuschert, S. J., Liu, Y. H. and Mallo, M. (1998). Hoxa-2 restricts the chondrogenic domain and inhibits bone formation during development of the branchial area. *Development* **125**, 2587-2597. doi:10.1242/dev.125.14.2587
Kmita, M., Tarchini, B., Zàkàny, J., Logan, M., Tabin, C. J. and Duboule, D. (2005). Early developmental arrest of mammalian limbs lacking HoxA/HoxD gene function. *Nature* **435**, 1113-1116. doi:10.1038/nature03648
Krumlauf, R. (1994). Hox genes in vertebrate development. *Cell* **78**, 191-201. doi:10.1016/0092-8674(94)90290-9
Lee, S., Remark, L. H., Josephson, A. M., Leclerc, K., Lopez, E. M., Kirby, D. J., Mehta, D., Litwa, H. P., Wong, M. Z., Shin, S. Y. et al. (2021). Notch-Wnt signal crosstalk regulates proliferation and differentiation of osteoprogenitor cells during intramembranous bone healing. *NPJ Regen. Med.* **6**, 29. doi:10.1038/s41536-021-00139-x
Leucht, P., Kim, J.-B., Wazen, R., Currey, J. A., Nanci, A., Brunski, J. B. and Helms, J. A. (2007). Effect of mechanical stimuli on skeletal regeneration around implants. *Bone* **40**, 919-930. doi:10.1016/j.bone.2006.10.027
Leucht, P., Kim, J.-B., Amasha, R., James, A. W., Girod, S. and Helms, J. A. (2008). Embryonic origin and Hox status determine progenitor cell fate during adult bone regeneration. *Development* **135**, 2845-2854. doi:10.1242/dev.023788
Liedtke, S., Buchheiser, A., Bosch, J., Bosse, F., Kruse, F., Zhao, X., Santourlidis, S. and Kögler, G. (2010). The HOX Code as a "biological fingerprint" to distinguish functionally distinct stem cell populations derived from cord blood. *Stem Cell Res.* **5**, 40-50. doi:10.1016/j.scr.2010.03.004
Lin, T.-Y., Gerber, T., Taniguchi-Sugiura, Y., Murawala, P., Hermann, S., Grosser, L., Shibata, E., Treutlein, B. and Tanaka, E. M. (2021). Fibroblast dedifferentiation as a determinant of successful regeneration. *Dev. Cell* **56**, 1541-1551.e1546. doi:10.1016/j.devcel.2021.04.016
Magli, M. C., Largman, C. and Lawrence, H. J. (1997). Effects of HOX homeobox genes in blood cell differentiation. *J. Cell. Physiol.* **173**, 168-177. doi:10.1002/(SICI)1097-4652(199711)173:2<168::AID-JCP16>3.0.CO;2-C
Magnusson, M., Brun, A. C. M., Miyake, N., Larsson, J., Ehinger, M., Bjornsson, J. M., Wutz, A., Sigvardsson, M. and Karlsson, S. (2007). HOXA10 is a critical regulator for hematopoietic stem cells and erythroid/megakaryocyte development. *Blood* **109**, 3687-3696. doi:10.1182/blood-2006-10-054676
Mark, M., Lufkin, T., Dolle, P., Dierich, A., LeMeur, M. and Chambon, P. (1993). Roles of Hox genes: what we have learnt from gain of function and loss of function mutations in the mouse. *C R Acad. Sci. III* **316**, 995-1008.
McNulty, C. L., Peres, J. N., Bardine, N., van den Akker, W. M. R. and Durston, A. J. (2005). Knockdown of the complete Hox paralogous group 1 leads to dramatic hindbrain and neural crest defects. *Development* **132**, 2861-2871. doi:10.1242/dev.01872
Morikawa, S., Mabuchi, Y., Kubota, Y., Nagai, Y., Niibe, K., Hiratsu, E., Suzuki, S., Miyauchi-Hara, C., Nagoshi, N., Sunabori, T. et al. (2009). Prospective identification, isolation, and systemic transplantation of multipotent mesenchymal stem cells in murine bone marrow. *J. Exp. Med.* **206**, 2483-2496. doi:10.1084/jem.20091046
Morris, S. A. (2016). Direct lineage reprogramming via pioneer factors; a detour through developmental gene regulatory networks. *Development* **143**, 2696-2705. doi:10.1242/dev.138263
Nogi, T. and Watanabe, K. (2001). Position-specific and non-colinear expression of the planarian posterior (Abdominal-B-like) gene. *Dev. Growth Differ.* **43**, 177-184. doi:10.1046/j.1440-169X.2001.00564.x
Orii, H., Kato, K., Umesono, Y., Sakurai, T., Agata, K. and Watanabe, K. (1999). The planarian HOM/HOX homeobox genes (Plox) expressed along the anteroposterior axis. *Dev. Biol.* **210**, 456-468. doi:10.1006/dbio.1999.9275
Owens, B. M. and Hawley, R. G. (2002). HOX and non-HOX homeobox genes in leukemic hematopoiesis. *Stem Cells* **20**, 364-379. doi:10.1634/stemcells.20-5-364
Papageorgiou, S. (2012). Comparison of models for the collinearity of hox genes in the developmental axes of vertebrates. *Curr. Genomics* **13**, 245-251. doi:10.2174/138920212800543093
Pineault, N., Helgason, C. D., Lawrence, H. J. and Humphries, R. K. (2002). Differential expression of Hox, Meis1, and Pbx1 genes in primitive cells throughout murine hematopoietic ontogeny. *Exp. Hematol.* **30**, 49-57. doi:10.1016/S0301-472X(01)00757-3
Pineault, K. M., Song, J. Y., Kozloff, K. M., Lucas, D. and Wellik, D. M. (2019). Hox11 expressing regional skeletal stem cells are progenitors for osteoblasts, chondrocytes and adipocytes throughout life. *Nat. Commun.* **10**, 3168. doi:10.1038/s41467-019-11100-4

Pinho, S., Lacombe, J., Hanoun, M., Mizoguchi, T., Bruns, I., Kunisaki, Y. and Frenette, P. S. (2013). PDGFRalpha and CD51 mark human nestin+ sphere-forming mesenchymal stem cells capable of hematopoietic progenitor cell expansion. *J. Exp. Med.* **210**, 1351-1367. doi:10.1084/jem.20122252

Rhoads, K., Arderiu, G., Charboneau, A., Hansen, S. L., Hoffman, W. and Boudreau, N. (2005). A role for Hox A5 in regulating angiogenesis and vascular patterning. *Lymphat. Res. Biol.* **3**, 240-252. doi:10.1089/lrb.2005.3.240

Roberts, S. J., Geris, L., Kerckhofs, G., Desmet, E., Schrooten, J. and Luyten, F. P. (2011). The combined bone forming capacity of human periosteal derived cells and calcium phosphates. *Biomaterials* **32**, 4393-4405. doi:10.1016/j.biomaterials.2011.02.047

Roberts, S. J., van Gastel, N., Carmeliet, G. and Luyten, F. P. (2015). Uncovering the periosteum for skeletal regeneration: the stem cell that lies beneath. *Bone* **70**, 10-18. doi:10.1016/j.bone.2014.08.007

Rossel, M. and Capecchi, M. R. (1999). Mice mutant for both Hoxa1 and Hoxb1 show extensive remodeling of the hindbrain and defects in craniofacial development. *Development* **126**, 5027-5040. doi:10.1242/dev.126.22.5027

Rux, D. R. and Wellik, D. M. (2017). Hox genes in the adult skeleton: Novel functions beyond embryonic development. *Dev. Dyn.* **246**, 310-317. doi:10.1002/dvdy.24482

Rux, D. R., Song, J. Y., Swinehart, I. T., Pineault, K. M., Schlientz, A. J., Trulik, K. G., Goldstein, S. A., Kozloff, K. M., Lucas, D. and Wellik, D. M. (2016). Regionally restricted Hox function in adult bone marrow multipotent mesenchymal stem/stromal cells. *Dev. Cell* **39**, 653-666. doi:10.1016/j.devcel.2016.11.008

Sakaguchi, Y., Sekiya, I., Yagishita, K. and Muneta, T. (2005). Comparison of human stem cells derived from various mesenchymal tissues: superiority of synovium as a cell source. *Arthritis. Rheum.* **52**, 2521-2529. doi:10.1002/art.21212

Schiedlmeier, B., Klump, H., Will, E., Arman-Kalcek, G., Li, Z., Wang, Z., Rimek, A., Friel, J., Baum, C. and Ostertag, W. (2003). High-level ectopic HOXB4 expression confers a profound in vivo competitive growth advantage on human cord blood CD34+ cells, but impairs lymphomyeloid differentiation. *Blood* **101**, 1759-1768. doi:10.1182/blood-2002-03-0767

Schwörer, S., Becker, F., Feller, C., Baig, A. H., Köber, U., Henze, H., Kraus, J. M., Xin, B., Lechel, A., Lipka, D. B. et al. (2016). Epigenetic stress responses induce muscle stem-cell ageing by Hoxa9 developmental signals. *Nature* **540**, 428-432. doi:10.1038/nature20603

Sela, Y., Molotski, N., Golan, S., Itskovitz-Eldor, J. and Soen, Y. (2012). Human embryonic stem cells exhibit increased propensity to differentiate during the G1 phase prior to phosphorylation of retinoblastoma protein. *Stem Cells* **30**, 1097-1108. doi:10.1002/stem.1078

Small, K. M. and Potter, S. S. (1993). Homeotic transformations and limb defects in Hox A11 mutant mice. *Genes Dev.* **7**, 2318-2328. doi:10.1101/gad.7.12a.2318

Song, J. Y., Pineault, K. M., Dones, J. M., Raines, R. T. and Wellik, D. M. (2020). Hox genes maintain critical roles in the adult skeleton. *Proc. Natl. Acad. Sci. USA* **117**, 7296-7304. doi:10.1073/pnas.1920860117

Studer, M., Lumsden, A., Ariza-McNaughton, L., Bradley, A. and Krumlauf, R. (1996). Altered segmental identity and abnormal migration of motor neurons in mice lacking Hoxb-1. *Nature* **384**, 630-634. doi:10.1038/384630a0

Svingen, T. and Tonissen, K. F. (2003). Altered HOX gene expression in human skin and breast cancer cells. *Cancer Biol. Ther.* **2**, 518-523. doi:10.4161/cbt.2.5.441

Taghon, T., Stolz, F., De Smedt, M., Cnockaert, M., Verhasselt, B., Plum, J. and Leclercq, G. (2002). HOX-A10 regulates hematopoietic lineage commitment: evidence for a monocyte-specific transcription factor. *Blood* **99**, 1197-1204. doi:10.1182/blood.V99.4.1197

Tapias, A., Zhou, Z.-W., Shi, Y., Chong, Z., Wang, P., Groth, M., Platzer, M., Huttner, W., Herceg, Z., Yang, Y.-G. et al. (2014). Trrap-dependent histone acetylation specifically regulates cell-cycle gene transcription to control neural progenitor fate decisions. *Cell Stem Cell* **14**, 632-643. doi:10.1016/j.stem.2014.04.001

Tarchini, B. and Duboule, D. (2006). Control of Hoxd genes' collinearity during early limb development. *Dev. Cell* **10**, 93-103. doi:10.1016/j.devcel.2005.11.014

Thorsteinsdottir, U., Sauvageau, G., Hough, M. R., Dragowska, W., Lansdorp, P. M., Lawrence, H. J., Largman, C. and Humphries, R. K. (1997). Overexpression of HOXA10 in murine hematopoietic cells perturbs both myeloid and lymphoid differentiation and leads to acute myeloid leukemia. *Mol. Cell. Biol.* **17**, 495-505. doi:10.1128/MCB.17.1.495

Thummel, R., Ju, M., Sarras, M. P., Jr and Godwin, A. R. (2007). Both Hoxc13 orthologs are functionally important for zebrafish tail fin regeneration. *Dev. Genes Evol.* **217**, 413-420. doi:10.1007/s00427-007-0154-3

Ugarte, F., Sousae, R., Cinquin, B., Martin, E. W., Krietsch, J., Sanchez, G., Inman, M., Tsang, H., Warr, M., Passegué, E. et al. (2015). Progressive chromatin condensation and H3K9 methylation regulate the differentiation of embryonic and hematopoietic stem cells. *Stem Cell Rep.* **5**, 728-740. doi:10.1016/j.stemcr.2015.09.009

van Gastel, N., Torrekens, S., Roberts, S. J., Moermans, K., Schrooten, J., Carmeliet, P., Luttun, A., Luyten, F. P. and Carmeliet, G. (2012). Engineering vascularized bone: osteogenic and proangiogenic potential of murine periosteal cells. *Stem Cells* **30**, 2460-2471. doi:10.1002/stem.1210

Wahba, G. M., Hostikka, S. L. and Carpenter, E. M. (2001). The paralogous Hox genes Hoxa10 and Hoxd10 interact to pattern the mouse hindlimb peripheral nervous system and skeleton. *Dev. Biol.* **231**, 87-102. doi:10.1006/dbio.2000.0130

Wang, W., Quan, Y., Fu, Q., Liu, Y., Liang, Y., Wu, J., Yang, G., Luo, C., Ouyang, Q. and Wang, Y. (2014). Dynamics between cancer cell subpopulations reveals a model coordinating with both hierarchical and stochastic concepts. *PLoS ONE* **9**, e84654. doi:10.1371/journal.pone.0084654

Wellik, D. M. and Capecchi, M. R. (2003). Hox10 and Hox11 genes are required to globally pattern the mammalian skeleton. *Science* **301**, 363-367. doi:10.1126/science.1085672

Winnik, S., Klinkert, M., Kurz, H., Zoeller, C., Heinke, J., Wu, Y., Bode, C., Patterson, C. and Moser, M. (2009). HoxB5 induces endothelial sprouting in vitro and modifies intussusceptive angiogenesis in vivo involving angiopoietin-2. *Cardiovasc. Res.* **83**, 558-565. doi:10.1093/cvr/cvp133

Wosczyna, M. N., Konishi, C. T., Perez Carbajal, E. E., Wang, T. T., Walsh, R. A., Gan, Q., Wagner, M. W. and Rando, T. A. (2019). Mesenchymal stromal cells are required for regeneration and homeostatic maintenance of skeletal muscle. *Cell Rep.* **27**, 2029-2035.e2025. doi:10.1016/j.celrep.2019.04.074

Yoshimura, H., Muneta, T., Nimura, A., Yokoyama, A., Koga, H. and Sekiya, I. (2007). Comparison of rat mesenchymal stem cells derived from bone marrow, synovium, periosteum, adipose tissue, and muscle. *Cell Tissue Res.* **327**, 449-462. doi:10.1007/s00441-006-0308-z

Yoshioka, K., Nagahisa, H., Miura, F., Araki, H., Kamei, Y., Kitajima, Y., Seko, D., Nogami, J., Tsuchiya, Y., Okazaki, N. et al. (2021). Hoxa10 mediates positional memory to govern stem cell function in adult skeletal muscle. *Sci. Adv.* **7**, eabd7924. doi:10.1126/sciadv.abd7924

Yue, R., Zhou, B. O., Shimada, I. S., Zhao, Z. and Morrison, S. J. (2016). Leptin receptor promotes adipogenesis and reduces osteogenesis by regulating mesenchymal stromal cells in adult bone marrow. *Cell Stem Cell* **18**, 782-796. doi:10.1016/j.stem.2016.02.015

Zhou, B. O., Yue, R., Murphy, M. M., Peyer, J. G. and Morrison, S. J. (2014). Leptin-receptor-expressing mesenchymal stromal cells represent the main source of bone formed by adult bone marrow. *Cell Stem Cell* **15**, 154-168. doi:10.1016/j.stem.2014.06.008